Dear Editor,

please find below our responses to the Reviewer's comments, that we upload again for your convenience, as well as the marked-up manuscript version, where all the changes we did are evidenced.

Kind Regards,

Manuela Volpe, on the behalf of the co-authors.

Dear Reviewers,

we thank you for your thoughtful comments. We addressed all of them as specified in detail in the point-to-point answers in the supplement pdf file, both in response to the general and to the specific comments of yours.

Here, we make some general remarks, since we made one important change in the revised manuscript. We also ask for a minor change to the title to insert in it the word “tsunami”, which was missing in the original title. This letter is repeated in all the three responses to the three Reviewers.

Changes to the results and to the manuscript.

We first of all need to point out that the change we made was necessary, since we found a bug in one of the numerical codes we had written for this study. This bug was found while performing some tests, some of them conceived for addressing your comments, particularly as far as the robustness and the importance of the correction for the near-field sources compared to the “noise” introduced by the tuning of the various filtering thresholds were concerned.

The bug consisted in a missing sum operator in the computation of the cluster probability (a missing cycle over one variable!). Hence, the probability of the entire cluster was not assigned to the cluster representative.

The new results, computed after the bug was corrected, do not differ in essence, although the resulting probabilities are obviously overall higher. All the new Figures are enclosed.

Conversely, for hazard intensities higher than 1 meter, the results now show even more pronounced differences between the “corrected” and “uncorrected” filtering procedures (new Figure 3c).

Our results now more clearly point out that not considering an appropriate correction for the near field would lead to overestimate the tsunami hazard. This is true in the case of this specific setting, though, since we found a prevalence of clusters causing coastal uplift from the near-field sources (the situation may be the opposite as well or a mix for different source-coast configuration).

These uplifts would tend to diminish tsunami inundation. Hence, the tsunami hazard would be overestimated without taking this into account. We hope this is illustrated by the new Figure 3c.

We now in fact added to panel c of this Figure a new quantity, that is the Mean Uplift (hereinafter MU) on a random point on the coastline in the inner - highest resolution - grid domain.

The MU provides the mean - over all scenarios contributing to some hazard intensities and all coastal points - co-seismic coastal displacement (with positive sign if uplift) plotted versus different hazard intensities, and it is compared to the relative percentage differences between the corrected and uncorrected results.

In more detail, the MU is obtained:

1. for the mean model - the same considered before as far as epistemic uncertainty is concerned;
2. for each single hazard intensity threshold, as said;
3. by performing a weighted average of the uplifts from each model (represented through the centroid of the cluster), where the weights are the annual probabilities of the individual models (of the individual earthquakes then), set to zero if the earthquake do not deform the coastline (i.e. for far-field sources) or if the tsunami doesn't exceed the given hazard intensity threshold; the weighted average is normalized to the total probability of the near- and far-field sources contributing to the tsunami hazard for that threshold;
4. by further averaging the result along the coastline, hence the MU may be interpreted as the mean on a random point of the coastline, from all the far-field and near-field scenarios, the latter including those causing both subsidence and uplift (note than that the absolute MU value in meters is then rather small being averaged over sources that cause either uplift or subsidence, or no coastal displacement at all).

Note that the intermediate results (before applying item 4.), that is the MU on each coastal point, for different intensity thresholds, both for single cluster representatives (red lines) and for the weighted average (according to item 3., blue line) are plotted in the new Figure S4. While we note that there are both positive and negative displacements (red lines corresponding to uplift and subsidence along the coast respectively), the predominant one is unveiled by the sum over the different clusters plotted (the a blue line).

Moreover, the results in Figure 3c now show very little differences between the "corrected" and "uncorrected" filtering procedures at low hazard intensities, that is those below the Filter H thresholds value of 1 meter.

In summary, for the specific case study, that is for this specific source-target configuration, our findings show that not considering an appropriate correction for near field would lead to overestimate the tsunami hazard for Hmax greater than 1m, and this overestimation is correlated to dominant coastal uplift. At lower intensities differences are small but not meaningful, as the results are biased by Filter H.

We will of course add the necessary new text in the revised manuscript concerning MU and the corresponding analysis.

New title.

We propose the following new title for this study: "From regional to local SPTHA: efficient computation of probabilistic **tsunami** inundation maps addressing near-field sources"
That is, we just inserted the word "tsunami" before inundation. This would make easier to find the article if searching NHESS for tsunami-related papers.

Kind Regards,
Manuela Volpe, on the behalf of the co-authors.

Response point-by-point to Anonymous Referee #1

The point-by-point answers are in blue color, below each Reviewer's comment (reported in *Italic*).

 # # Overall comments #

This looks to be a good paper about an important topic that is of clear interest to NHESS readers. It is mostly well written, and describes innovative ideas which are likely to be of broad utility in tsunami hazard assessment.

- *My only 'significant' concern is that the authors do not provide a 'conceptual justification' for the differences in the results of the two filtering methods they apply, for the case of high H_{max}. As it stands, as a reader I don't know why this happens. Intuitively the reasons are not obvious, and as it relies on some rather delicate calculations (which we know are sensitive to choices of coefficients in filters, etc). At the moment I cannot be confident that the results are 'stable' enough to justify the conclusion that "it is important to distinguish near and far-field sources in the filtering approach". If the authors can provide some 'conceptual backing' to support these results, then in my judgement the paper should clearly be accepted for publication in NHESS. In saying this, please note that I accept the fact that some aspects of these filtering approaches cannot be completely stable (e.g. in the authors example, results with H_{max} < 1m are not meaningful). This is expected, and not a problem. However, they need to provide more justification that the results at higher return periods are stable enough to justify the key conclusion.*

(the answer below is the same for a similar question from Reviewer 2)

The conceptual explanation traces back to the fact that the two procedures are not equivalent from a physical point of view and we could roughly say that one is in principle “correct” and the other one is “wrong”. Maybe in saying "it is important to distinguish near and far-field sources in the filtering approach" we were not clear enough. What we wanted to stress is that a blind filtering procedure based on offshore tsunami amplitudes produces a non representative selection of the important scenarios, as it could aggregate or even remove important local scenarios.

We try to explain it better below.

In the original procedure by Lorito et al., offshore tsunami amplitudes are supposed to be representative of the coastal inundation, regardless of the source location with respect to the coast. That was reasonable, since it considered either far field scenarios with respect to the coast of Sicily, or scenarios which deformed the coast of Crete Island always in the same direction, since they were all subduction earthquake on the neary Hellenic Arc.

Indeed, offshore tsunami profiles could be strongly misleading when coseismic deformation of the coast occurs, either as coastal uplift or subsidence depending on the causative earthquake. The coseismic displacement induced by local earthquakes can modify the actual onshore tsunami intensity corresponding to the same offshore wave. Hence, near field scenarios must be separately treated, and clustered considering the source similarities, including the co-seismic coastal displacement, rather than the offshore tsunami wave similarity.

We will try to report these “conceptual” arguments in the revised manuscript as concisely as possible.

The tuning of the thresholds in the filtering procedure is a different task, but we note that the same thresholds have been used with and without the correction for near field, so that the differences we found in the results obtained from the two procedures are not in our opinion imputable to those choices.

On the other hand, we can now support such conceptual justification providing the physical explanation of the specific results, based on the new quantity MU (mean uplift) we calculated and described in our introductive general remarks. This also answers to one of your specific comments below.

In general, lower ‘corrected’ hazard means that the predominant effect by local sources contributing to a specific point on the hazard curve - that is to the probability of exceedance for a given intensity threshold - is represented by coastal uplift, which in turn decreases tsunami hazard. In other words, there is a prevalence of clusters represented by scenarios causing uplift. Conversely, higher hazard would correspond to coastal subsidence.

As we said, we investigated this aspect, computing, for different intensity thresholds above 1m, the MU on a random point along the coastline of the inner grid, produced by near field representative scenarios contributing to the hazard at that threshold, weighted by the occurrence probability associated to each scenario (corresponding to the probability of the entire cluster it represents) and normalized to the probability of all of the scenarios contributing to the same intensity threshold.

The obtained positive values, although not representative of the real coastal displacement as averaged on all the scenarios (including that ones which do not produce appreciable coseismic local deformation), indicate that the dominant contribution to the coseismic deformation is an uplift of the coast, in agreement with the percentage differences retrieved between the two approaches.

We hope to have answered in this way to the “significant” concern expressed by the Reviewer. We must acknowledge that this comment made us deepen the analysis and consider our results much more carefully - and indeed we found a bug.

Specific comments

- *P7, around line 10: I think you mean that you neglect a bunch of ’other’ important sources of uncertainty, but, you do comprehensively test the filtering procedure (?? right?? – actually upon reading the full paper I’m still uncertain). At the moment the paragraph doesn’t make it clear if your example is actually a ’strong’ evaluation of the filtering procedure, given the idealized assumptions on the source. Please make* *this clearer.*

The test site illustrative application is not a real hazard assessment, as it is based on a quite rough probability model as well as on some strong assumptions regarding the filtering thresholds and the source modeling.

Nevertheless, although relatively simplified, our source model is still quite complex, and includes even epistemic uncertainties on many source parameters, e.g concerning the seismic rates, the shape of the magnitude-frequency distribution, even the seismogenic depth for the two considered subduction zones, and several others. It also includes ensemble uncertainty modeling. We now include a new Figure in the Supplementary Materials (Figure S2), which should make clearer that the model deals with epistemic uncertainty, as it shows the comparison between the mean offshore hazard curves at selected points along the 50m isobath (see Figure 2a of the manuscript), as well as the comparison between some quantiles of the epistemic uncertainty, for the filtered and original set of scenarios. Please refer to Selva et al. 2016 for further details on the adopted source model.

So, we consider the model as fully suitable to test and describe the procedure. We anyway restate that the aim of the application is to highlight that inaccurate (biased) evaluation of site-specific tsunami hazard would be obtained if scenarios located in the near field of the target area are not properly taken into account, irrespectively of the completeness and consequent complexity of the hazard assessment. A “real” application would be just more complicated and more computationally demanding.

- P8, top of page – it would be good to report on some sensitivity analysis of this to give the reader a ’feel’ for how severe these approximations are (e.g. you could halve the number of clusters, so you don’t have to do more simulations).

The filtering procedure surely introduces some approximations and ideally the goal should be to reduce the computational cost of PTHA while keeping the error with respect to the whole set of sources as small as possible. In the present work, considering the illustrative nature of the case study, we enlarged the accepted error to further reduce the number of explicit numerical simulations.

First of all, the most severe approximation was made during the filtering on tsunami amplitude: it goes without saying that a threshold of 1m might be not acceptable in case of a real hazard assessment, while it is an acceptable threshold for illustrative purposes. It is worth stressing that this filter, independently from the threshold value, does not affect subsequent steps of the procedure, as it represents a rigid cut-off of the number of scenarios we are accounting for.

Another strong assumption was made regarding the cluster analysis: the k-medoids partitioning algorithm is based on the minimization of the sum of the intra-cluster distances, i.e. the distances between each element of a cluster and the cluster centroid. Strong constraints on the distances result in a more accurate partitioning, in terms of similarity between the elements of each cluster, but lead to a great number of clusters. Instead, larger ranges of acceptability increase the efficiency of the algorithm, in terms of number of resulting clusters, to the detriment of the accuracy.

As an example, we provide here a sensitivity analysis on the threshold imposed on the intra-cluster variance (step (3a)): the new Figure S3 shows the relative differences in absolute value between the offshore (i.e. at the control points along the 50m isobath) hazard curves computed from the complete initial set of sources and the filtered set (at the end of the cluster analysis). The red box corresponds to the threshold value we chose (0.2): it appears evident that a smaller value would have allowed a stronger constraint on the error introduced by the cluster analysis, while considerably increasing the number of resulting clusters. Vice versa, higher thresholds produce a smaller number of clusters, but fail in reproducing the hazard (error up to 40%). Our choice in our opinion represented the best trade off for our purposes. Again, in case of a real hazard assessment, the lower threshold would be likely better.

- *P8, bottom of page – 'it is worth noting that results at H_{max} < 1m ...' – OK, but because those results are not meaningful, can you please 'clip' your figure limits so that they do not include H_{max} < 1m. That will help the reader focus on parts of the curve that you do consider meaningful, and ease the interpretation of the figures.*

We apologise as we have misspoken: what we intended is that the hazard curves below 1m can be (negatively) biased since they are depleted from the scenarios removed by Filter H. Following your suggestion, we rephrased and shadowed that part of the plots in Figure 3. This depletion is also clearly observed in new Figure S2 for low amplitudes.

- *P9, paragraph around lines 10-15 – It's not evident to me why method 3a should 'over-estimate' rates for H_{max}>3 (or indeed why the difference is reversed at lower H_{max}). Can you give a heuristic explanation of why this could happen? Without some idea of this, my thinking is 'maybe a calculation/convergence type error' (!). Or is it that, for large enough H_{max}, the associated local sources have a greater tendency to be filtered than the distant ones, for some reason – and the converse for smaller H_{max}? Definitely not obvious to me – please discuss it.*

As discussed before, a lower hazard at a certain point of the hazard curve, due to the near field correction, means that the coseismic field from local sources that dominate the hazard produces a coastal uplift. We agree this was not sufficiently proved before, but the new Figure (3c), with the MU superimposed to the percentage differences between the two approaches now should better illustrate that the overestimation is correlated to the dominant coastal uplift.

- *P9, paragraph around line 5 – I agree that you've shown that a 'blind' cluster analysis might produce quite different results from the 2-stage approach proposed in the paper. However, I'm less confident about the stability of either procedure. Can you really say that the 2-stage approach is better, based on the results presented here? Consider the following "devil's advocate" theory – from what you've presented, I hypothesis that "Both of your approaches are strongly affected by the details of the filtering coefficients, and equally big differences could be expected from merely adjusting those in reasonable ranges". In other words, how can readers be confident that the results are not just 'noise'? Probably you can justify this, but I don't see it from the current text. So please add in some discussion that explains 'why' these results happen, and why you expect them to be 'basically robust' {notwithstanding that you have to make some severe approximations for low events – that's ok – but* *at least for high events, we need some conceptual explanation of the results}.*

As it should be clear now from our previous answers, involving the new Figure 3 and MU, there are firm conceptual reasons supporting the need of a “2-stage approach”. You are indeed right that the results are stronger for larger amplitudes. This is clearer with the new results.

The simplest explanation remains though the same: the original assumption that offshore tsunami amplitudes are representative of the coastal inundation may fail if local sources producing appreciable coseismic deformation of the coast - of conflicting sign, i.e. some uplift and some subsidence depending on the source - are involved.

Hence, one (the only?) way we can take this into account is to separate near and far field scenarios and treat local sources removing the approximation introduced by the cluster analysis on the tsunami amplitudes, since offshore profile can not be considered reliable for such sources. This considerations hold irrespectively of the stability of the results in our example. However, our results “behave” as expected, being dependent on the approach used.

Indeed, the near field treatment is still an approximation, as we reduced the number of numerical simulations with respect to the “exact” case, by performing a cluster analysis based on the coseismic fields. However, it should be a better approximation with respect to aggregate local and remote scenarios on the basis of the offshore tsunami amplitudes.

Moreover, our application is also aimed to investigate if such procedure is really needed from the point of view of results, that is if, apart from the physical meaning of the procedure, results are actually affected by the near field correction.

The fact that the contribution from the near field turned out to be significant, even investigating a target site with relatively low near-field tsunamigenic seismicity, was not straightforward.

We finally stress that the two approaches (with or without the correction for near field) only differ in the way local sources are treated: the filtering coefficients are basically consistent. In other words, the different results can not be related to the filtering thresholds.

We repeat, the “conceptual explanation”, should now be there with the new results and the new analysis presented. And we must acknowledge that this comment was really useful.

➢ P11, line 6 – as mentioned above, please provide more ’conceptual explanation’ as to why this happens.

As extensively discussed in the previous answers, this is related to the coseismic deformation induced by local sources, which, if properly accounted, modify the effective tsunami hazard.

Detailed comments

➢ P3, L31 – suggest changing ’is released’ to ’is not used’.

- P5, L5: – suggest changing ’will produce as well similar inundation patterns’ to ’will also produce similar inundation patterns’.
- P5, lines 6-7 – Please provide the equation for the cost function. I looked up the 2010 paper, but it appears to refer to time-series comparisons rather than H-max comparisons. Better to make it very obvious to the reader.
- P6, around lines 10-11 – It’s not clear to me how you use the co-seismic deformation as a metric for source-proximity in the cluster analysis. Ahh, I see you do this below around lines 25. Give that, please add "(details below)" at the end of the sentence that finishes on line 11.
- P7, line 20 – there is a number with multiple ’.’ inside – this is not familiar notation to me, do you intend to use some other separator?

We thank for your suggestions, which will be all addressed in the revised manuscript. In particular, we will clarify that the cost function equation firstly introduced in the 2010 papers to compare time series while solving inverse problems was modified by Lorito et. al 2015 for Hmax comparison.

Response point-by-point to Anonymous Referee #2

The point-by-point answers are in blue color, below each Reviewer's comment (reported in *Italic*).

##General comments##

This paper addresses an important topic, namely the development of onshore probabilistic tsunami hazard assessments and overcoming the related computational challenges. It builds on the work of Lorito et al. 2015 and Selva et al. 2016. A key innovation in this study is efficient filtering of near-field sources based on coseismic deformation, rather than offshore tsunami wave height. Overall, the paper is well written and concisely explains the issues and methods used to overcome them, and is suitable for publication in NHESS with some minor revisions.

In reviewing the paper, my main suggestions (details given below) are:

1. *Siting the introduction more broadly in the PTHA literature. While this paper builds directly on the work of Lorito et al. 2015 and Selva et al. 2016, which is heavily relied upon in the introduction, along with the review paper by Grezio et al 2017, there are a number of additional relevant papers related to PTHA problems that could be cited. In my opinion, this would more neatly place this paper within the broader context of PTHA literature, widening the appeal of the paper. I.e. this paper should be framed as a step forward in PTHA in general, not just an update of the Lorito and Selva methods (although it is that too).*

We fully agree and appreciate the suggestion. Citing Lorito et al. 2015 and Selva et al. 2016 was indeed mandatory. Conversely, using only Grezio et al. 2017 to refer to PTHA was certainly too simplistic. We will improve the bibliography to better frame the paper in the context, also following your specific suggestions below.

As a result, we added the following references, including also those stemming from other comments below:

Brizuela, B., Armigliato, A., and Tinti, S. (2014). Assessment of tsunami hazards for the central american pacific coast from southern mexico to northern peru. Natural Hazards and Earth System Sciences, 14(7):1889–1903.

Burbidge, D., Cummins, P. R., Mleczko, R., and Thio, H. K. (2008). A probabilistic tsunami hazard assessment for western australia. Pure Appl. Geophys., 165(11):2059–2088.

Davies, G., Griffin, J., Løvholt, F., Glimsdal, S., Harbitz, C., Thio, H. K., Lorito, S., Basili, R., Selva, J., Geist, E., and Baptista, M. A. (2017). A global probabilistic tsunami hazard assessment from earthquake sources. Geological Society, London, Special Publications, 456.

Gailler, A., Calais, E., Hebert, H., Roy, C., and Okal, E. (2015). Tsunami scenarios and hazard assessment along the northern coast of haiti. Geophysical Journal International, 203(3):2287–2302.

Geist, E. L. (2002). Complex earthquake rupture and local tsunamis. Journal of Geophysical Research: Solid Earth, 107(B5):ESE 2–1–ESE 2–15.

Griffin, J. D., Pranantyo, I. R., Kongko, W., Haunan, A., Robiana, R., Miller, V., Davies, G., Horspool, N., Maemunah, I., Widjaja, W. B., Natawidjaja, D. H., and Latief, H. (2017). Assessing tsunami hazard using heterogeneous slip models in the Mentawai Islands, Indonesia. Geological Society of London Special Publications, 441:47–70.

Gusman, A. R., Tanioka, Y., MacInnes, B. T., and Tsushima, H. (2014). A methodology for near-field tsunami inundation forecasting: Application to the 2011 tohoku tsunami. Journal of Geophysical Research: Solid Earth, 119(11):8186–8206.

Harbitz, C., Glimsdal, S., Bazin, S., Zamora, N., Løvholt, F., Bungum, H., Smebye, H., Gauer, P., and Kjekstad, O. (2012). Tsunami hazard in the caribbean: Regional exposure derived from credible worst case scenarios. Continental Shelf Research, 38:1 – 23.

Horspool, N., Pranantyo, I., Griffin, J., Latief, H., Natawidjaja, D. H., Kongko, W., Cipta, A., Bustaman, B., Anugrah, S. D., and Thio, H. K. (2014). A probabilistic tsunami hazard assessment for indonesia. Nat. Hazards Earth Syst. Sci., 14(11):3105–3122.

Løvholt, F., Bungum, H., Harbitz, C. B., Glimsdal, S., Lindholm, C. D., and Pedersen, G. (2006). Earthquake related tsunami hazard along the western coast of thailand. Natural Hazards and Earth System Sciences, 6(6):979–997.

Power, W., Wang, X., Wallace, L., Clark, K., and Mueller, C. (2017). The New Zealand probabilistic tsunami hazard model: development and implementation of a methodology for estimating tsunami hazard nationwide. Geological Society, London, Special Publications, 456.

Satake, K., Fujii, Y., Harada, T., and Namegaya, Y. (2013). Time and space distribution of coseismic slip of the 2011 tohoku earthquake as inferred from tsunami waveform datatime and space distribution of coseismic slip of the 2011 tohoku earthquake. Bulletin of the Seismological Society of America, 103(2B):1473.

2. *Some assessment of the sensitivity to the choices made in the filtering process (i.e. choice of thresholds etc) and whether this has any implication to the broader conclusions. Also whether it is possible for biases to be introduced in this process.*

(the answer below is the same for a similar question from Reviewer 1)

The conceptual explanation traces back to the fact that the two procedures are not equivalent from a physical point of view and we could roughly say that one is in principle “correct” and the other one is “wrong”. Maybe in saying "it is important to distinguish near and far-field sources in the filtering approach" we were not clear enough. What we wanted to stress is that a blind filtering procedure based on offshore tsunami amplitudes produces a non representative selection of the important scenarios, as it could aggregate or even remove important local scenarios.

We try to explain it better below.

In the original procedure by Lorito et al., offshore tsunami amplitudes are supposed to be representative of the coastal inundation, regardless of the source location with respect to the coast. That was reasonable, since it considered either far field scenarios with respect to the coast of Sicily, or scenarios which deformed the coast of Crete Island always in the same direction, since they were all subduction earthquake on the neary Hellenic Arc.

Indeed, offshore tsunami profiles could be strongly misleading when coseismic deformation of the coast occurs, either as coastal uplift or subsidence depending on the causative earthquake. The coseismic displacement induced by local earthquakes can modify the actual onshore tsunami intensity corresponding to the same offshore wave. Hence, near field scenarios must be separately treated, and clustered considering the source similarities, including the co-seismic coastal displacement, rather than the offshore tsunami wave similarity.

We will try to report these “conceptual” arguments in the revised manuscript as concisely as possible.

The tuning of the thresholds in the filtering procedure is a different task, but we note that the same thresholds have been used with and without the correction for near field, so that the differences we found in the results obtained from the two procedures are not in our opinion imputable to those choices.

On the other hand, we can now support such conceptual justification providing the physical explanation of the specific results, based on the new quantity MU (mean uplift) we calculated and described in our introductive general remarks. This also answers to one of your specific comments below.

In general, lower ‘corrected’ hazard means that the predominant effect by local sources contributing to a specific point on the hazard curve - that is to the probability of exceedance for a given intensity threshold - is represented by coastal uplift, which in turn decreases tsunami hazard. In other words, there is a prevalence of clusters represented by scenarios causing uplift. Conversely, higher hazard would correspond to coastal subsidence.

As we said, we investigated this aspect, computing, for different intensity thresholds above 1m, the MU on a random point along the coastline of the inner grid, produced by near field representative scenarios contributing to the hazard at that threshold, weighted by the occurrence probability associated to each scenario (corresponding to the probability of the entire cluster it represents) and normalized to the probability of all of the scenarios contributing to the same intensity threshold.

The obtained positive values, although not representative of the real coastal displacement as averaged on all the scenarios (including that ones which do not produce appreciable coseismic local deformation), indicate that the dominant contribution to the coseismic deformation is an uplift of the coast, in agreement with the percentage differences retrieved between the two approaches.

We hope to have answered in this way to the “significant” concern expressed by the Reviewer. We must acknowledge that this comment made us deepen the analysis and consider our results much more carefully - and indeed we found a bug.

3. *Some comment on whether other metrics besides maximum tsunami height or co-seismic deformation could be relevant in assigning events to clusters.*

Yes, sure. This might be certainly relevant, at least for far-field sources. Storing and using the full waveforms, or considering maybe periods and polarities, or other approaches, can be considered.

Take into account though that this was already briefly discussed in Lorito et al. 2015. It was tested there that after some tuning of the length of the offshore profile of control points, the offshore height profile turned out to be a sufficiently good indicator for approximating the inundation afterwards. We may speculate that this is due to the collective information provided by the maximum heights themselves taken altogether, which then becomes a kind of maximum wave profile. Nevertheless, we will briefly discuss the issue in the revised manuscript, also using the examples you provide in your specific comment.

Vice-versa, as far as near-field sources are concerned, two modelled tsunamis with very similar sources should be quite similar, except in case of a very sensitive dependence on initial conditions - like for the butterfly-effect. We are not totally convinced but we will cautiously mention the issue in the revised manuscript.

In addition, there are several minor areas for clarification to improve the communication of the results, and a few grammatical errors.

##Specific comments##

1. Introduction
As mentioned above, this could benefit from reference to broader PTHA literature, specifically:

- *P2L4: Should also cite other PTHA studies as incremental gains in uncertainty quantification have been made over the past decade or so. Include Burbidge et al 2008; Gonzalez et al 2009; Horspool et al 2014; Davies et al 2017, Power et al 2017 (there may be others).*
- *P2L7-8: These references (Geist and Lynett 2014; Grezio et al 2017) are not the first to emphasise computational approaches to PTHA – see additional references suggested in the above point.*
- *P2L10: Should also reference Davies et al. 2017 regarding uncertainty quantification.*
- *P2L13: Gonzalez et al 2009 should be cited in reference to challenges of PTHA for inundation.*
- *P2L16: Geist 2002 should also be mentioned here.*
- *P2L17. Mueller et al 2014 and Griffin et al. 2015 have both undertaken on-shore tsunami hazard assessments considering heterogeneous earthquake rupture;*

although neither was fully probabilistic, they should be mentioned here as first steps towards quantifying this uncertainty for inundation hazard. Both also discuss the effect of coseismic displacement on onshore hazard and how this can vary locally, as discussed on P3L2. Here (P3L2) the discussion could be expanded to provide greater justification to your methodological approach to near field hazard.

These references provide as said a broader context to the paper and we already listed above those we will include in the revised manuscript.

We will improve the introduction accordingly, following all your suggestions, for the different categories, such as: the uncertainty quantification, the computational approaches, challenges for PTHA inundation, rupture complexity and near-field, coseismic displacement and onshore hazard.

➢ *P1L20: This isn't true. In practice many inundation assessments also use 'representative scenarios' for a range of return periods, not just 'worst credible'.*

We will clarify the statement, adding the mention to "representative scenarios" and some appropriate references - listed above as well, mostly using some scenarios for different representative recurrence times sometimes combined with worst case ones, that is: Gailler et al. 2015; Harbitz et al. 2012; Løvholt et al. 2006; Brizuela et al., 2014.

➢ *P1L22: One or a limited range of inundation scenarios get used for much more than 'a first screening' by emergency managers. These scenarios regularly get used to develop emergency management plans, evacuation plans, undertake impact assessments and so on. In my opinion this paragraph severely underplays the utility of scenario hazard assessments. The main problem is that we can't translate the offshore probability to an onshore probability. I expect that even with probabilistic inundation hazard maps, single event scenarios will still be used for a range of emergency management scenario planning purposes – we'll just be in a position to actually say what the probability of the event in terms of inundation hazard is.*

Here we need to disagree a bit; or better, this is not what we meant, since we also wrote: "to realize very detailed assessments of specific scenarios." This goes beyond the "first screening", in our intention. We will clarify this in the revised manuscript, also referring to disaggregation of PTHA for selecting physically meaningful individual scenarios. Instead, we are sorry but we are not sure we understand the statement "we can't translate the offshore probability to an onshore probability.", since in this paper - as well as in other papers from different authors - fully probabilistic inundation maps are presented.

➢ *P2L20: Need to clarify that this is talking about onshore PTHA – offshore PTHA are in general computationally affordable (though not cheap!) these days.*

Agree, we will modify the text accordingly.

➢ *P2L30: 'while solving all the emerging technical and scientific issues'. This seems a fairly bold claim! Perhaps rephrase.*

We apologise for the misunderstanding: it was intended to emphasize that the work also concerned the implementation of the procedure, which was not trivial. We will rephrase according to your comment.

2. Method outline This section is clear and well-written

3. Implementation of an improved filtering methodology

- *P5L4-5: How confident are you in the assumption that similar wave heights lead to similar onshore hazard? What about other wave properties such as period, which may be significant in determining onshore behaviour. E.g. Satake et al 2013 showed how inundation from the Tohoku tsunami was variably controlled by long-period components on flat coastal plains and shorter-period peaks in steep coastal areas. While set within a tsunami warning context rather than hazard assessment context, Gusman et al 2014 used two cycles of a tsunami waveform in identifying 'similar' tsunami. I think some of the issues are resolved for near field tsunami in your coseismic deformation filtering approach presented following, but it could still be good to comment on this issue here.*

We generally agree and we have responded to the related general comment 3. above. We nevertheless give some specific answers here, partly repeating our previous answer.

The general assumption that, for a given source, offshore tsunami amplitude profiles are representative of the coastal inundation behind was applied and tested in the previous work by Lorito et. al (2015). On the other hand, we agree that caution must be used as well, since the previous paper did not deepen into any possible specific case.

Indeed we faced for example the problem when treating near field scenarios, as you observed.

We also agree that there might be other issues. As said the wave period is an important property controlling the tsunami impact: in fact, we someway accounted for that by considering a control profile along the target coast, advancing a kind of ergodic hypothesis.

Future developments of our method could take into account a Gusman-like approach, considering the tsunami time history at each point of the control profile, instead of just the maximum wave height. We will nevertheless add a few comments about this in the manuscript adopting the suggested line of reasoning. We thank you for pointing this out.

- *P6L30-35: It is not entirely clear how the distance is measured across the grid of coseismic deformation points, and how the spatial component is handled – perhaps also write the relevant equation to ensure clarity.*

The comparison between the coseismic deformation fields is carried out point-to-point. The squared Euclidean distance is the metric used for the cluster analysis and only the vertical components are taken into account. We will try and rephrase for the sake of clarity.

4. The Milazzo oil refinery

- *P8L28: The abbreviation Mmax is very commonly used to mean the maximum magnitude for a given earthquake source in seismic and tsunami hazard assessment. I would suggest changing this to something else to avoid confusion.*

We will change this MFmax (maximum momentum flux). This will appear as well in the new Figures (those after correcting the results for the bug) in the Supplementary Materials.

- *P9L11: This should be 'overestimates the probability for a given Hmax relative to STEP (3b).*

Ok, we will modify the sentence as suggested.

- *P9L23: Should these be >=, not =, if you're talking about probabilities of exceedance.*

Probability maps are obtained by vertically "cutting" the hazard curves for each point of the grid, i.e. representing on a map the exceedance probability values for a fixed H_{max} . In this sense, the "=" sign is correct. We will add the "(exceedance)" in parentheses before probability for clarity.

- *P9L26-30: Use of phrase 'positive' and 'negative differences' is confusing and makes the meaning of the paragraph somewhat ambiguous. Better to rephrase stating more explicitly which model gives relatively higher/lower hazard etc.*

We agree that the sentences are quite unclear; we will rephrase them referring more explicitly to higher/lower hazard.

- *Also, the difference between results far inland, near the coast and offshore in Figure 4a need to be explained. Why the shift from negative to positive differences at some distance inland from the coast?*

We first need to point out that Figure 4 has changed based on the new results.

We assume that you are referring to the Figure with the differences between the probability maps for steps 3a and 3b and for the intensity threshold of 2 meters (the top right one). We apologise for the confusion and we will add labels where missing to all Figures.

However, note that now this Figure is quite different from before, as it contains more positive values. This is consistent with the new Figure 3c, where the differences are already positive for this threshold and even larger for the 3 metres threshold.

As far as the negative inland values are concerned, note that they occur for very low probability values. So, maybe they shouldn't be overinterpreted. We will however comment all the new Figures based on the new results in the revised manuscript.

- *P10L5: Can anything additional be said about possible biases in the sampling process? Why is it likely that the sampling produced a non-representative selection of the important scenarios? How does this overall affect the strength of you conclusions in comparing the two methods (i.e. could the differences be random rather than systematic).*

What we meant here is that without the correction for near field, namely without a separate treatment for remote and local sources, the filtering procedure provides a non-representative selection of the important scenarios.

This is due to the basic assumption that offshore tsunami amplitudes can be considered representative of the onshore tsunami impact, which surely introduces a bias when the scenarios which deform the coastline are not separated by those that doesn't do it (step (3a)).

For example, admit that 2 different scenarios will both produce 1 meter wave offshore. However, one scenario uplifts the coast of 1 meter, the other one creates 1 meter subsidence. The two inundations will be dramatically different, but the two scenarios would be nevertheless grouped by (3a) under the same cluster.

Therefore, the procedure proposed as step (3b) is in principle the correct one to evaluate site-specific tsunami hazard, when local effects of coseismic deformation can not be neglected.

5. Conclusions

- *P10L10: The statement around the definition of the source scenarios seems a bit strong. I'd suggest removing the word 'fully' as I doubt this has really been done. Aleatory uncertainty applies to both the rate model and the source location, geometry, maximum magnitude etc. I'd suggest putting 'and their mean annual rates' prior to 'exploring source uncertainty'.*

We agree with the comment: the word "fully" here is misleading. Although in principle the proposed methodology allow us for a full exploration of the aleatory uncertainty, some practical limitations are always present in real life. We will correct the text accordingly.

- *P10L19: Suggest 'from offshore wave amplitudes alone'. Also, what about other parameters such as period for non near-field tsunami? This links back to my comments on Section 3.*

Ok, got it, we'll rephrase by saying only that it is unlikely that the assumption holds if there is co-seismic coastal displacement.

Figures:

- *Figure 1: Step 2 should read 'tsunami propagation to offshore points'*
- *Figures 3-5 need labels for parts a), b) etc.*

OK, we added labels where missing in the new figures.

##Technical corrections##

- Throughout: Why use STEP instead of Step?
- P1L11: demonstrate not demonstrated
- P2L25: Rephrase to 'This allows identification of a subset of ...'

- P2L29: Rephrase to ‘Here we merge the two approaches of Lorito et al....’
- P3L21: Change ‘resume’ to ‘summarise’. Also P10L9
- P4L8: Change ‘enough representative’ to representative enough’
- P6L10: Change ‘and a separate modelling’ to ‘and separate modelling’
- P6L34-35: Change to ‘while the stopping criterion is based on the Euclidean distance’
- P7L16: Mediterranean Sea (not sea)
- P8L1: Replace ‘Namely’ with ‘That is’; delete ‘even’
- P8L25: Please specify the shear modulus used for the Okada calculations
- P9L15: Remove ‘supposedly’
- P10L24: Change ‘has not to be’ to ‘is not’.
- P11L3-4: I think this should read ‘As a consequence, the effect of coastal deformation on tsunami hazard can not be deduced...’
- P11L14: Change to ‘...the approach developed here allows consideration of a very high number...’

We thank you for these technical corrections, which will be all addressed in the revised manuscript. Concerning the Okada calculations, a poissonian solid is assumed with $\lambda=\mu$, so that the Okada results are independent of the shear modulus.

Response point-by-point to Anonymous Referee #3

The point-by-point answers are in blue color, below each Reviewer's comment (reported in *Italic*).

Overview: The authors did an extension of the SPTHA method previously proposed by Lorito et al. (2015) [GJI] and Selva et al. (2016) [GJI]. A new filtering scheme for earthquake scenarios is developed (Filter P) and the method is applied to a particular coast (Milazzo).
Overall evaluation: The application of the SPTHA to a new region and adding some innovations to the previously-developed method may justify publication of this work The paper is not as good as the other two papers published before (I mean Lorito et al. 2015; Selva et al. 2016). The current manuscript refers to the previous two papers very frequently and does not seem to stand by its own. However, I am positive about this work and I think it can be published in NHESS after some revisions. I made some suggestions below.

We thank for your positive evaluation. Our manuscript in fact does not propose a totally new method, but develops an upgrade of the method previously proposed by the cited published papers. This is the reason for frequently referring to them.

Comments:

- *Page 3, "Method": your Section 2 looks a review of the methods previously published by Lorito et al. (2015) [GJI] and Selva et al. (2016) [GJI]. Your own method is outlined in Section 3. This is confusing. In fact, your current section 2 is sort of literature review. I suggest change the title of Section 2 to "A review of SPTHA" and then change title of Section 3 to "Methods: an improved SPTHA".*

We understood the point, although Section 2 is not properly a literature review of SPTHA but just a summary of the original method. Anyway, we will provide more suitable titles. For example, they might be: "A review of the original method" for Section 2 and "Improvements in the filtering procedure" for Section 3.

- *To show the better performance of the new method over the ones published before (I mean Lorito et al. 2015; Selva et al. 2016), a discussion or a figure is needed.*

The improved method, illustrated in Figure 1 of our manuscript, fits into the general scheme displayed in Figure 1 of Selva et al. 2016, who already foresaw the possibility of performing site specific tsunami hazard, although they did not addressed nor implemented or tested it.

The performances of the "new" method step (3b) are here benchmarked with respect to step (3a), which corresponds to the original method as, although including some improvements, it lacks the most crucial novelty, that is the separate treatment of the near-field scenarios. It is discussed in several places that this was not done by Lorito et al. 2015. We will consider if stressing this again while summarizing the results.

- *Try not to refer to two previous papers so much. You may want to show more independence.*

Ok, we will remove the references where possible.

- *In Page 9, refer to appropriate figures when discussing the results.*

We agree, and will modify accordingly.

- *Why you have capital letters for STEP? Is that necessary? If not, change it to "step" because when you use capital letters, the reader assumes it is an acronym. I guess it is not an acronym for anything.*

We did not consider possible confusion with an acronym. As capital letters are not really necessary here, we will change it.

- *Page 5, Line 17: explain more about Filter P.*

Filter P is further explained by lines 17-29. We will try to make it clearer in the revised version.

- *Page 6, Line 2: what is intra-cluster? It is unclear. Make sure to explain more about it and clarify how it works.*

Intra-cluster variance means the variance within each cluster; it was used in the original method to define the optimal number of cluster in the cluster analysis procedure, according to the so-called Beale test. This will be better explained in the revised text.

- *Page 6, Line 7: delete statements like "as mentioned before..." it is not suitable for academic writing.*
- *Page 7, Line 32: delete "as discussed in previous ...." Again not suitable*.

We accept the comments and will revise accordingly

- *Page 8: here you use "cluster" and "scenario" interchangeably. Make sure which one you meant. I assume that you meant "Scenario" not "cluster". They are different. Cluster is much bigger than a single scenario. One cluster can include 200 scenarios. In Line 13, you say: "We obtained 634 and 520 clusters for remote and local sources, respectively, that is a total of 1154 scenarios ...". Here the sum of 634 and 520 clusters cannot be 1154 scenarios. Instead, the sum of 634 and 520 clusters cannot be 1154 CLUSTERS.*

There is no doubt that "cluster" and "scenario" are two different things. At the end of the cluster analysis we obtain clusters of scenarios, but for each cluster a representative scenario is selected, to which the probability of occurrence of the entire cluster is assigned, and then the representative scenarios are the ones which are explicitly modeled. In this sense a certain number of clusters corresponds to the same number of scenarios to be simulated. We will clarify in the text.

- Your conclusion has many repeats; for example lines 8-13. Make sure delete all repeats.

- ABSTRACT: try to have more numbers and conclusions, not only generic statements.
- CONCLUSIONS: shorten it to a paragraph and be specific and do not repeat all stuff again.

We will take into account the above general style suggestions in the revised text, thank you.

- *Figure 1: The last box repeats. Delete one of them.*

The last box, relative to step (4) is repeated twice in order to highlight that step (3a) and (3b) are completely separate paths. In our opinion, reporting step (4) just once, connected both to step (3a) and (3b) is misleading, as it could suggest a “merging” of the results of simulations from the two paths to evaluate SPTHA.

- *Figure 2: Explain what are two sets of red dots.*

We agree: this information is missing in the figure caption. We will correct.

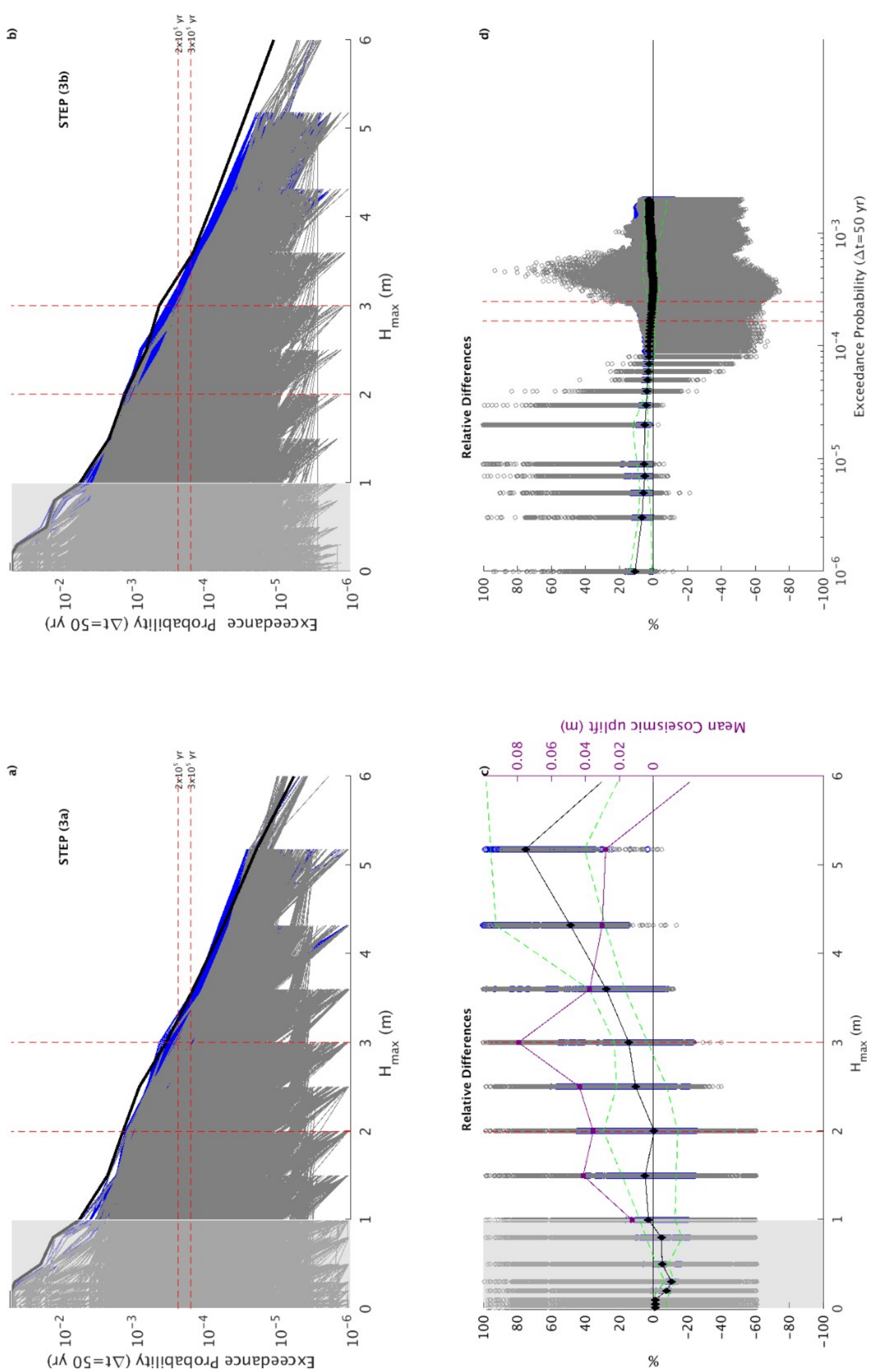

fig. 3 nel papero

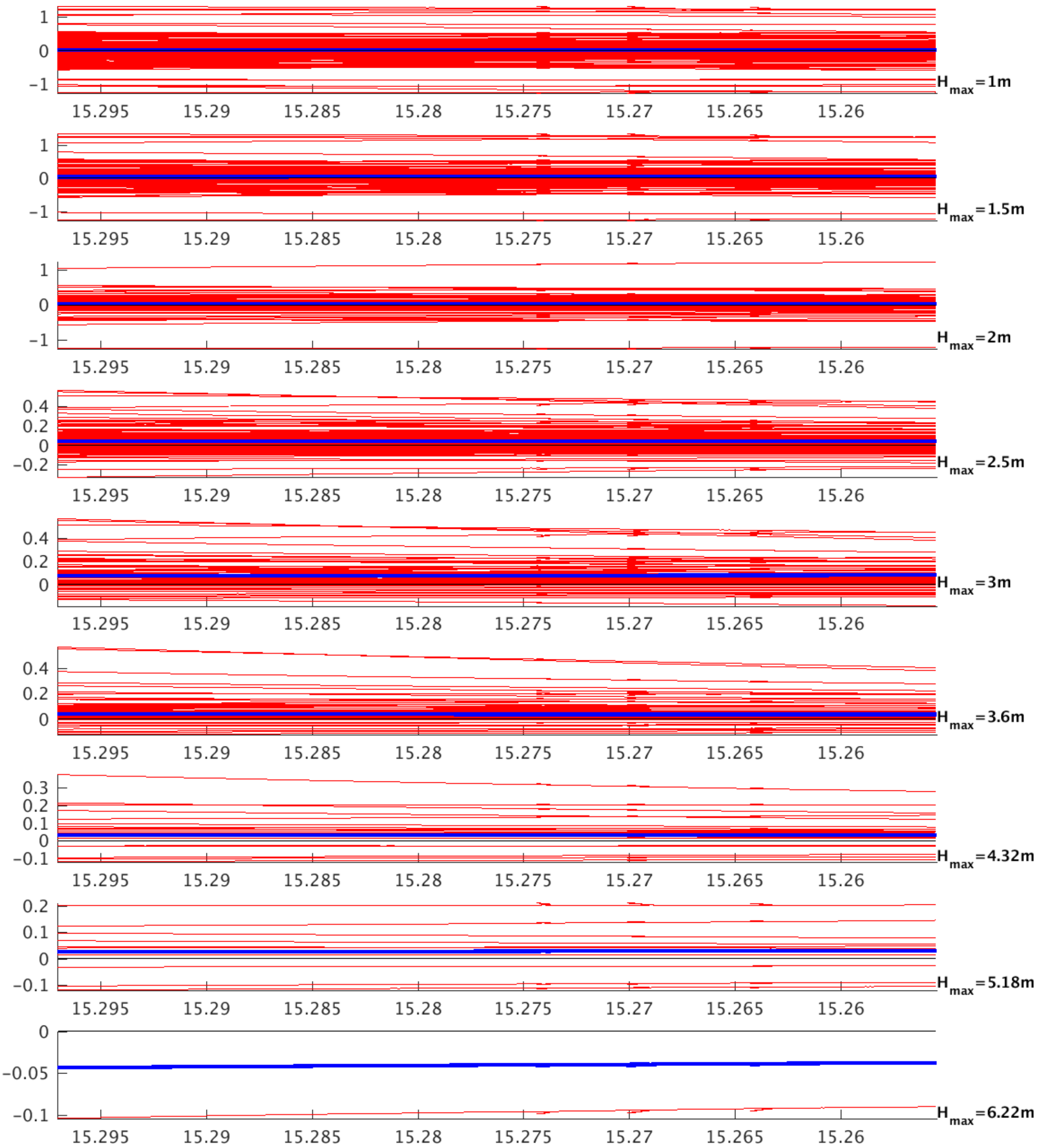

H_max=1m
H_max=1.5m
H_max=2m
H_max=2.5m
H_max=3m
H_max=3.6m
H_max=4.32m
H_max=5.18m
H_max=6.22m

fig. new1

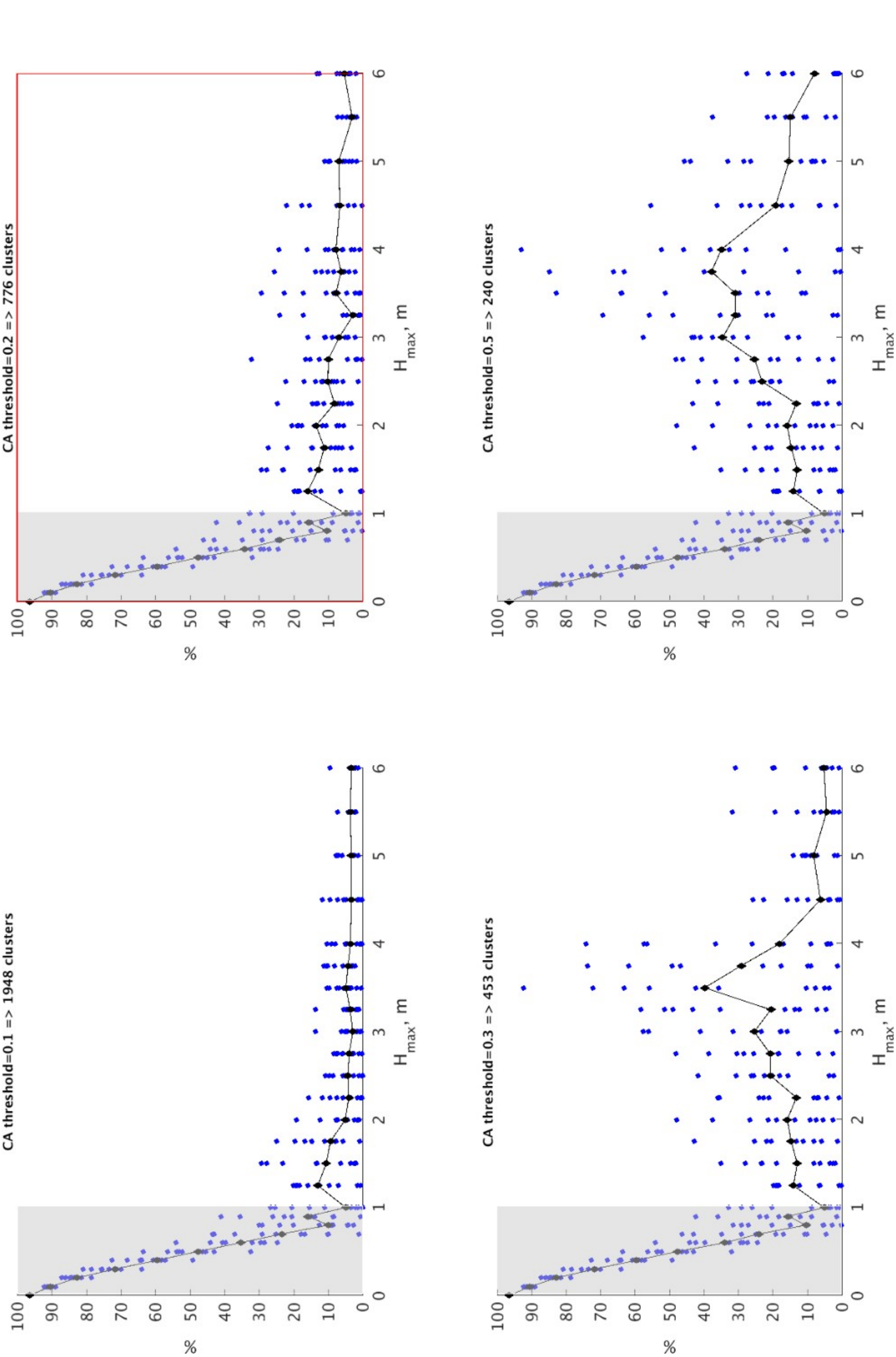
CA threshold=0.1 => 1948 clusters
CA threshold=0.2 => 776 clusters
CA threshold=0.3 => 453 clusters
CA threshold=0.5 => 240 clusters
%
H_{max}, m

fig. new2

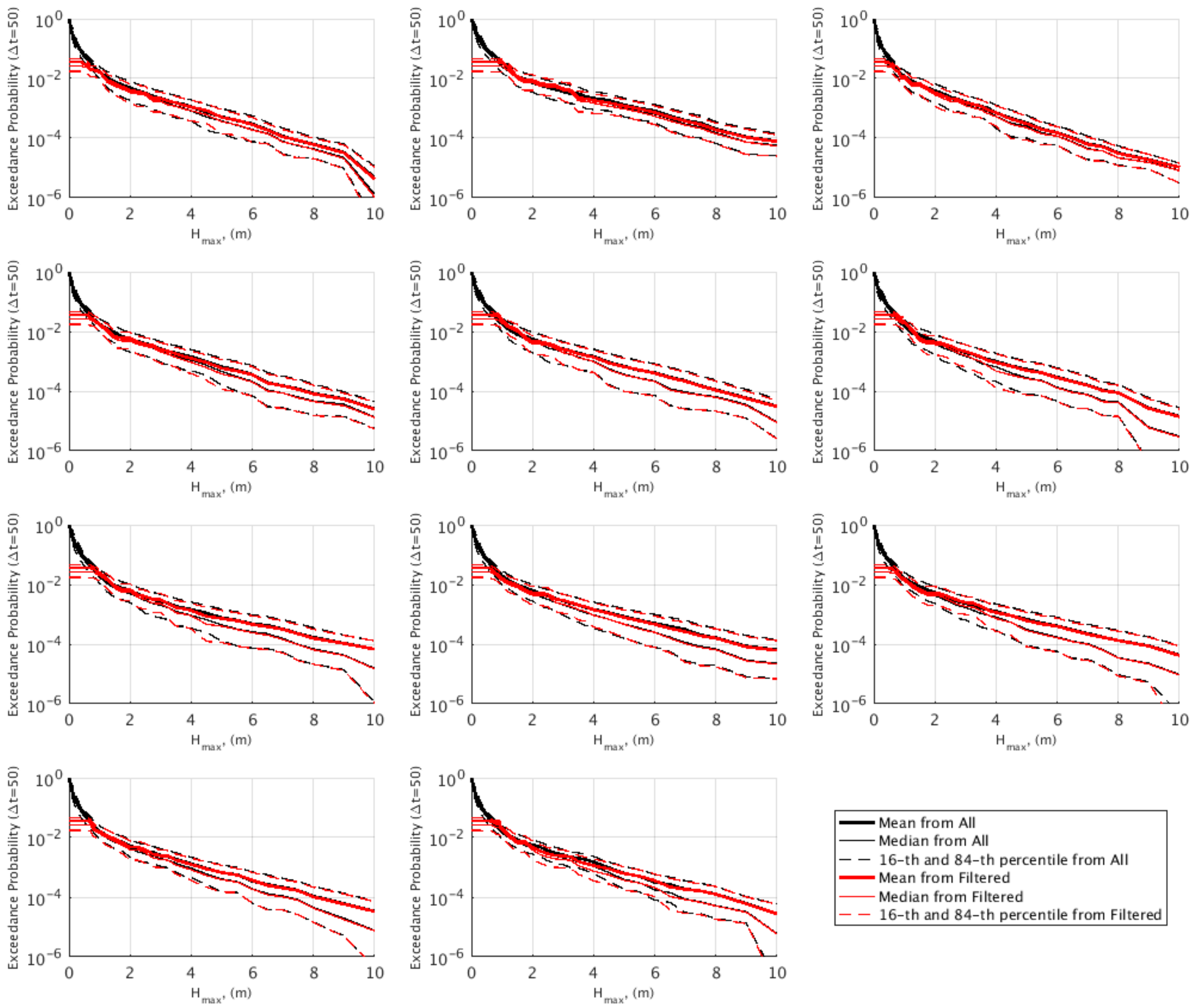

Exceedance Probability (Δt=50)
H_max, (m)
Mean from All
Median from All
16-th and 84-th percentile from All
Mean from Filtered
Median from Filtered
16-th and 84-th percentile from Filtered

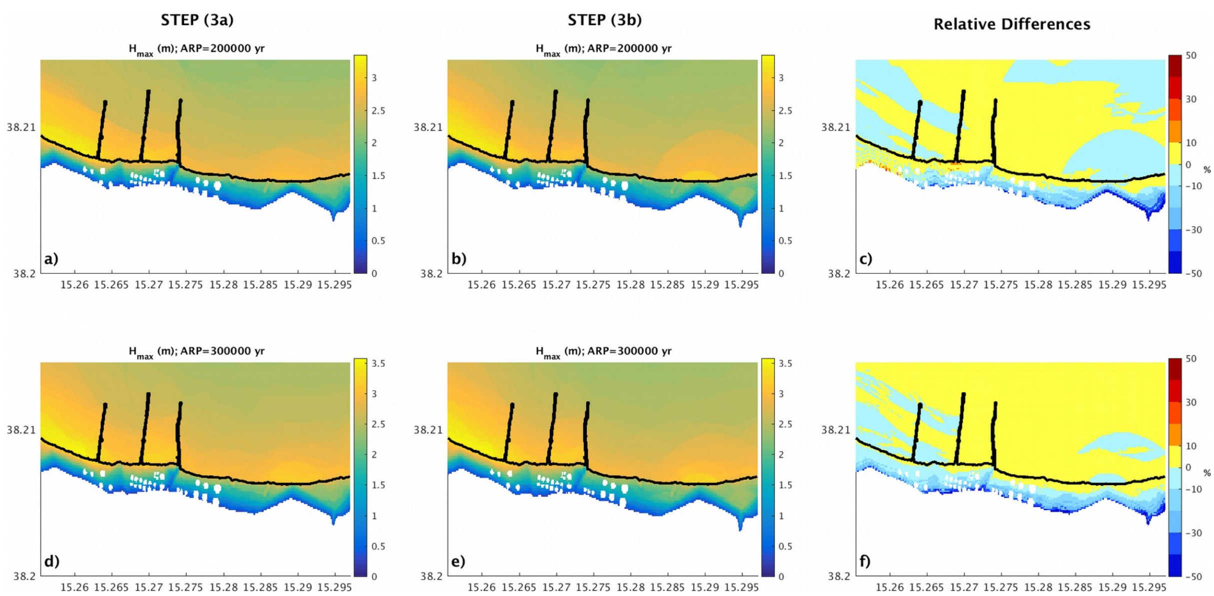

STEP (3a)
STEP (3b)
Relative Differences
H_max (m); ARP=200000 yr
H_max (m); ARP=300000 yr
a)
b)
c)
d)
e)
f)
%

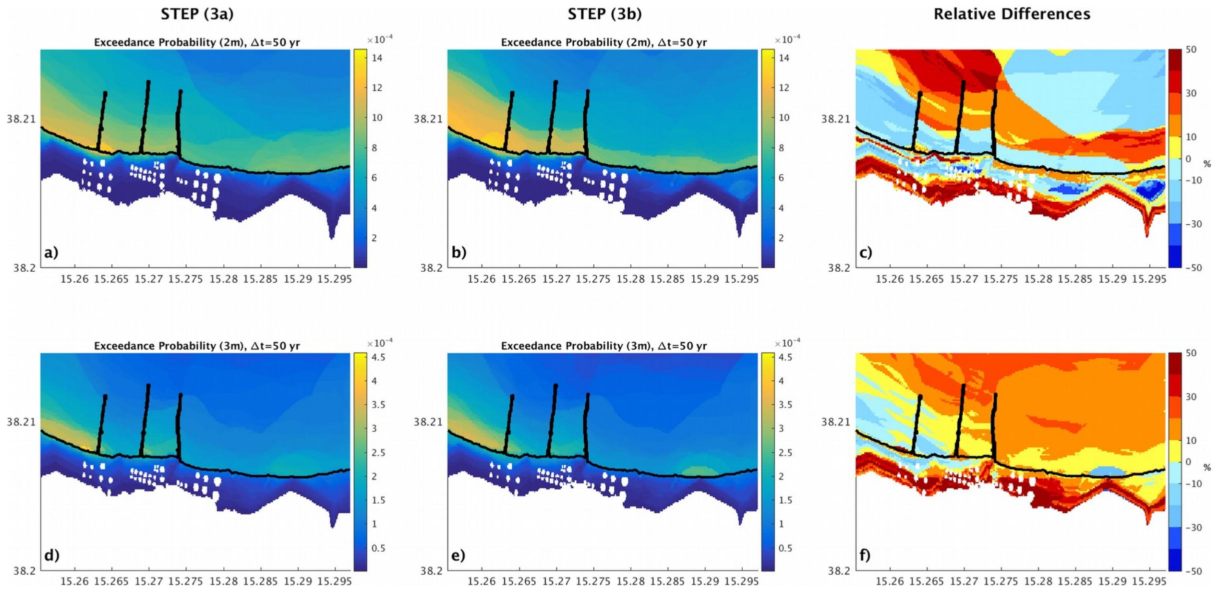

STEP (3a)
STEP (3b)
Relative Differences
Exceedance Probability (2m), Δt=50 yr
Exceedance Probability (3m), Δt=50 yr
a)
b)
c)
d)
e)
f)
38.21
38.2
15.26 15.265 15.27 15.275 15.28 15.285 15.29 15.295
×10⁻⁴
%

From regional to local SPTHA: efficient computation of probabilistic tsunami inundation maps addressing near-field sources

Manuela Volpe, Stefano Lorito, Jacopo Selva, Roberto Tonini, Fabrizio Romano, and Beatriz Brizuela
Istituto Nazionale di Geofisica e Vulcanologia, Italy
Correspondence: M. Volpe (manuela.volpe@ingv.it)

Abstract. Site-specific Seismic Probabilistic Tsunami Hazard Analysis (SPTHA) is a computationally demanding task, as it requires in principle a huge number of high-resolution numerical simulations for producing probabilistic inundation maps. We implemented an efficient and robust methodology using~~that, based on the similarity of offshore tsunamis and hazard curves in front of a target site, uses~~ a filtering procedure to reduce the number of numerical simulations needed, while still allowing full treatment of aleatory and epistemic uncertainty. Moreover, we developed a strategy to identify~~near-field sources are identified~~, on the basis of the tsunami ~~coseismic~~ initial conditions, and separately treat near-field scenarios,~~treated~~ to avoid biases in the tsunami hazard assessment. Indeed, the ~~In fact, coastal~~ coseismic deformation produced by local earthquakes necessarily affects the tsunami intensity, depending on the scenario size, mechanism, and position, as coastal uplift or subsidence tend to diminish or increase the tsunami hazard, respectively. Therefore, we proposed~~developed~~ two parallel filtering schemes in the far- and the near-field, based on the similarity of offshore tsunamis and hazard curves and on the coseismic fields, respectively. This becomes mandatory as~~For near-field sources~~ offshore tsunami amplitudes can not represent a proxy for the coastal inundation in case of near-field sources~~, and filtering is based on coseismic field~~. We applied the method to an illustrative use-case at the Milazzo oil refinery (Sicily, Italy). We demonstrate that a blind filtering procedure can not properly account for local sources and would lead to a non representative selection of the important scenarios. For the specific source-target configuration, this results into an overestimation of the tsunami hazard, which turns out to be correlated to dominant coastal uplift. Different settings could produce either the opposite or a mixed behavior along the coastline. However, we show that the effects of the coseismic deformation due to local sources can not be neglected and a suitable correction has to be employed when assessing local scale SPTHA, irrespectively of the specific sign of coastal displacement.~~By comparison of the results obtained with and without the correction for the near-field sources, for a use-case at the Milazzo oil refinery (Sicily, Italy), we demonstrate that special treatment of local sources plays a fundamental role and is applicable in local scale SPTHA.~~

1 Introduction

In the last fifteen years, a number of large earthquakes, often accompanied by destructive tsunamis, occurred worldwide. In several cases, the overall size of the earthquake and/or of the tsunami was unanticipated and some surprising features were observed, in terms of event scaling (e.g., source aspect ratio, tsunami height versus earthquake magnitude) or associated damage (Lay, 2015; Lorito et al., 2016); a striking example is the 2011 Tohoku earthquake and tsunami and the consequent nuclear disaster at the Fukushima Dai-ichi power plant (Synolakis and Kânoğlu, 2015). These events called the attention for a systematic re-evaluation of current tsunami hazard estimates.

In the past, tsunami hazard was mostly studied through simulations of one or several scenarios, either “worst credible” (e.g., Tinti and Armigliato, 2003; Lorito et al., 2008; Tonini et al., 2011; Løvholt et al., 2012a) or representative for different selected return periods (e.g., Løvholt et al., 2006; Harbitz et al., 2012; Brizuela et al., 2014; Gailler et al., 2015)~~“worst credible” earthquake scenarios and the associated tsunami~~. Such an approach can be useful either as a first screening of tsunami hazard~~to inform emergency managers on the potential of tsunamis and their features~~ or to realize very detailed assessments to inform emergency managers on the potential impact of specific scenarios. Traditionally, the latter is often done also as a result of probabilistic hazard disaggregation (Bazzurro and Cornell, 1999).

To account for the tsunami potential variability ~~of the phenomena associated to tsunamis~~ and ~~their~~ frequency, and for including~~of the eventual~~ alternative models needed for quantifying the epistemic uncertainty, the probabilistic treatment of a large set of potential tsunami sources is essential. Probabilistic Tsunami Hazard Analysis (PTHA) probably begun with the seminal papers of Lin and Tung (1982) and Rikitake and Aida (1988). Uncertainty quantification is one of the main goals of PTHA, and progressively more refined uncertainty treatment was achieved following the 2004 Indian Ocean tsunami~~the Probabilistic Tsunami Hazard Analysis (PTHA)~~ (e.g., Geist and Parsons, 2006; Burbidge et al., 2008; González et al., 2009; Horspool et al., 2014; Hoechner et al., 2016; Selva et al., 2016; Davies et al., 2017; Grezio et al., 2017; Power et al., 2017). PTHA~~, which~~ is becoming the~~more and more~~ established ~~as a~~ good practice to manage risk assessment and risk mitigation measures (Chock et al., 2016; Løvholt et al., 2017). Due to the lack of historical tsunami data, the opportunity to deal with PTHA through a computational approach, involving the probability of all of the relevant sources and the numerical modeling of the generated tsunamis, which is in the scope of all the above mentioned papers, is~~has been recently~~ emphasized for example by several reviews (Geist and Lynett, 2014; Grezio et al., 2017). ~~This allows, for example, to account for the relative contributions of large and small events at different mean annual rates and, even more important, to attain a quantitative treatment of the uncertainty (e.g., Selva et al., 2016; Grezio et al., 2017).~~

Nevertheless, the computational procedure for a complete evaluation of PTHA, fully honoring the natural variability of the sources, can be extremely demanding and unfeasible in some cases, particularly when inundation calculations are involved for a target site (González et al., 2009; Geist and Lynett, 2014). This is due to the very large number of numerical simulations of tsunami generation, propagation and inundation on high resolution topo-bathymetric models which is, in principle, required. For example, numerous realizations of heterogeneous slip are needed and usually obtained with stochastic procedures (LeVeque et al., 2016; Sepúlveda et al., 2017). Indeed, heterogeneous earthquake slip is known to strongly influence the tsunami run-up (Geist, 2002; Løvholt et al., 2012b; Geist and Oglesby, 2014; Davies et al., 2015; Murphy et al., 2016), not only in the the near-field of the source (Li et al., 2016). Among some first attempts towards quantifying tsunami hazard uncertainty related to heterogeneous earthquake slip~~Actually~~, Mueller et al. (2014) and Griffin et al. (2017) should be mentioned. Recently, Goda and De Risi (2018) proposed a multi-hazard approach including stochastic slip distributions and cascading earthquake-tsunami risk evaluation; however they considered a limited number of tsunami scenarios, without fully characterizing the epistemic uncertainties associated with the key model components. Consequently, an efficient methodology is needed to make (onshore) PTHA a computationally affordable task.

The issue has been dealt with in various ways in several studies (González et al., 2009; Thio et al., 2010; Lorito et al., 2015; Lynett et al., 2016). In particular, Lorito et al. (2015) focused on Seismic PTHA (SPTHA), that is on hazard associated to tsunamis generated by coseismic seafloor displacement. They developed a method for significantly reducing the computational cost of the assessment, by means of a source filtering procedure based on a cluster analysis. This allows the identification of~~to identify~~ a subset of important sources able to preserve the accuracy of results. Furthermore, Selva et al. (2016) proposed a general procedure for the joint and unbiased quantification of the aleatory and epistemic uncertainty, including the filtering procedure by Lorito et al. (2015) while stressing the importance of source completeness.

Here, we merge~~deepen into the merging of~~ the two approaches by Lorito et al. (2015) and Selva et al. (2016), fully developing a method that enables the quantification of the local scale SPTHA, also devoting a big effort in refining the procedure~~while solving all the emerging technical and scientific issues~~ and introducing several critical improvements. On one hand, we modified the filtering procedure to enhance its computational efficiency and to adapt it to multiple sources covering a large range of source-target distances. On the other hand, to improve the accuracy, we applied a separate treatment for remote and local sources, selecting near-field scenarios on the basis of the similarity of the coseismic tsunami initial conditions. This is crucial, as near-field sources may challenge the general assumption made by Lorito et al. (2015), where, for a given source, offshore tsunami amplitude profiles are considered representative of the coastal inundation behind, regardless of the source location with respect to the coast. It was reasonable in that case study, since they considered either far-field scenarios with respect to the target coast or scenarios which deformed the coast in a definite direction, that is the coast always subsided due to subduction earthquakes on the Hellenic Arc. In the presence of more complex (and realistic) local fault distribution, causing either subsidence or uplift or mixed patterns depending on the cases,~~: indeed, coastal uplift or subsidence due to the coseismic displacement induced by local earthquakes can modify the actual~~ tsunami intensity~~, which~~ can be unpredictably reduced or enhanced with respect to the corresponding offshore tsunami wave~~by nearby the target area~~ (Mueller et al., 2014; Griffin et al., 2017). Hence, in general, offshore tsunami profiles could be strongly misleading when coseismic deformation of the coast occurs. This may in particular affect~~is particularly important to preserve~~ the tail of the hazard curves (i.e. largest intensities), to which local sources significantly contribute, as also demonstrated by the disaggregation analysis in Selva et al. (2016). For all these reasons~~this reason~~, a special treatment is needed for local sources, based on the source similarities considering the coseismic onshore displacement, rather than the offshore tsunami wave similarity.

For illustrative purposes, we considered, as a use-case, a target site in the Central Mediterranean, that is the Milazzo oil refinery (Sicily, Italy), in the Southern Tyrrenian sea. This site was previously selected within the framework of the EU project

STREST (http://www.strest-eu.org/) as a test case for multi-hazard stress test development for non-nuclear critical infrastructures.

It is worth noting that this paper is strictly methodological and is aimed to propose a computationally efficient procedure for local scale SPTHA, rather than providing a realistic site-specific hazard assessment. In fact, for the sake of simplicity and in order not to deflect the attention from the core of the method, no efforts have been dedicated to constrain and test the (regional) seismic rates, the local seismic sources and their geometry and dynamics, including slip distributions, as well as the accuracy of topo-bathymetric data used in tsunami simulations. Moreover, the filtering procedure has been forced to minimize the number of explicit numerical simulations, allowing a relatively larger accepted error with respect to the complete initial set of sources due to the introduced approximations.

The paper is organized as follows: section 2 resumes the general outline of the method for SPTHA evaluation, as proposed by Lorito et al. (2015) and Selva et al. (2016), while the innovative developments are described in section 3; section 4 focuses on the illustrative application; conclusive remarks are drawn in section 5.

2 A general review of the original method for SPTHA~~Method outline~~

Using regional scale SPTHA as input for local scale (site-specific) SPTHA, through the approach proposed by Lorito et al. (2015), is a task already foreseen by Selva et al. (2016) (see Fig. 1 therein). However, this possibility was neither applied nor tested in practice, since their main focus was the application to regional scale analyses. The details of the general method have been already thoroughly described and validated in the previous studies. Here we will summarize~~resume~~ the basic concepts.

The whole general procedure for site specific SPTHA can be outlined in four steps: (1) the definition of earthquake scenarios and their probability, allowing in principle a full exploration of source aleatory uncertainty; (2) the computation, for each source, of tsunami propagation up to a given offshore isobath; (3) the selection of the relevant scenarios for a given site through a filtering procedure and the relative high-resolution tsunami inundation simulations; (4) the assessment of local SPTHA with joint aleatory and epistemic uncertainty quantification by means of ensemble modeling, including modeling alternatives eventually implemented at steps (1)-(3).

In step (1), all the modeled earthquakes must be defined for different seismic regions, which are assumed to be independent from each other. The earthquake parameters and their logically ordered conditional probabilities are treated by means of an event tree technique. We emphasize that the common assumption that tsunami hazard is dominated at all time scales by subduction zone earthquakes is not used: non-subduction faults, unknown offshore faults and diffuse seismicity around major known and well mapped structures are all taken into account. This strategy attempts to prevent biases in the hazard due to incompleteness of the source model (Basili et al., 2013; Selva et al., 2016). The seismicity related to the main and better known fault interfaces is treated separately from the rest of the crustal and diffuse seismicity. A similar approach has been used in the recent TSUMAPS-NEAM project (http://www.tsumaps-neam.eu), which provided the first SPTHA model for the North-Eastern Atlantic, Mediterranean and connected seas (NEAM) region.

In step (2), for each scenario retrieved from step (1), the corresponding tsunami generation and propagation is numerically modeled, and the pattern of offshore tsunami ~~wave~~ height above the sea level (H_{max}) is evaluated on a set of points along the $50m$ isobath, in front of the target area. To provide the input to Lorito et al. (2015), these points may be limited to a profile in front of the site. The length of this control profile must be tuned depending on the morphology and the extension of the target coast: a trade-off has to be reached, as few points could make the profile not representative enough, while too many points could downgrade the performances of the subsequent filtering procedure (Lorito et al., 2015). Actually, the optimal length is the shortest one that makes the offshore hazard curves stable with respect to the source selection, and further increase in length would increase the computational effort without significantly altering the results.

In step (3), using the offshore H_{max} profiles calculated at step (2), a filtering procedure is implemented to select a subset of relevant sources, based on the similarity of the associated tsunami intensity, not on the similarity or spatial proximity of the sources themselves. The selected sources, each of them representative of a cluster of sources producing comparable tsunamis offshore the target area, are then used for explicit inundation modeling on high-resolution topo-bathymetric grids. This approach allows for a consistent and significant reduction of the computational cost, while preserving the accuracy. However, Lorito et al. (2015) considered a limited set of sources. The extension to a much larger set of potential sources requires some modification to the method that, along with several other improvements, are proposed in this study, as reported in section 3.

Incidentally, we note that other wave properties such as period or polarity could be relevant in the framework of the cluster analysis. However, Lorito et al. (2015) briefly discussed this issue, also with respect to the length of the control profile as discussed above. Nevertheless, this is a point probably deserving further investigation, considering that Satake et al. (2013) showed how inundation from the Tohoku 2011 tsunami was variably controlled by long-period offshore tsunami components on flat coastal plains and shorter-period peaks in steep coastal areas. Indeed, Gusman et al. (2014) used two cycles of a tsunami for identifying similar waves. Conversely, since, as described in the next section, offshore wave comparison is not here used anymore in the near-field, this issue will not apply for local sources.

In step (4), local SPTHA is quantified. The inundation maps for each representative scenario from step (3) are aggregated according to the probabilities provided at step (1), assigning the total probability of a cluster to the representative scenario. Aleatory and epistemic uncertainty are simultaneously quantified by means of an ensemble modeling approach (Marzocchi et al., 2015; Selva et al., 2016) over alternative implementations of the previous steps. In practice, steps (1) to (3) can be iterated for each alternative model and these alternatives can be weighted according to their credibility and the possible correlations among the models. The results are finally integrated through ensemble modeling into a single model which expresses both aleatory and epistemic uncertainty.

3 Improvements in the filtering procedure~~Implementation of an improved filtering methodology~~

The described method has been tested by both Selva et al. (2016) and Lorito et al. (2015). However, Lorito et al. (2015) focused on the filtering procedure of step (3), adopting a simplified configuration for the source variability, in which sources were allowed only within the Hellenic arc, that is an area relatively smaller than the full aleatory variability. On the other hand, Selva et al. (2016) applied the approach to a regional study extended to the Ionian Sea, in Central Mediterranean. The quantification of the local hazard is instead discussed only in theory, without proposing any application.

The original method by Lorito et al. (2015) adopted a two-stage procedure.

In the first stage, scenarios giving a negligible contribution to H_{max} offshore the target area were removed, assuming they would lead to negligible inundation. Hereinafter, we call this stage "Filter H".

As a second filtering stage, a Hierarchical Cluster Analysis (HCA) was carried out, separately for each earthquake magnitude class included in the seismicity model, under the assumption that sources producing~~which produce~~ similar offshore H_{max} along the control profile will also produce ~~as well~~ similar inundation patterns. The distance between two H_{max} patterns from~~, that is between~~ two different scenarios u and v was measured by a cost function previously used to compare tsunami waveforms in source inversion studies (e.g., Lorito et al., 2010; Romano et al., 2010) and modified by Lorito et al. (2015) as

$$d(H^u_{max}, H^v_{max}) = \left[1 - \frac{2\sum_x H^{u,x}_{max} H^{v,x}_{max}}{\sum_x (H^{u,x}_{max})^2 + (H^{v,x}_{max})^2}\right], \tag{1}$$

where x runs over the control points on the $50m$ isobath. For each cluster, the scenario closer to the centroid was selected as the reference scenario, with an associated probability corresponding to the probability of occurrence of the entire cluster. The optimal number of clusters (i.e., the "stopping criterion") was assessed by analyzing the variance within each cluster (hereinafter "intra-cluster")~~intra-cluster variance~~ as a function of the number of clusters and selecting the largest value still producing significant changes, according to the so-called Beale test (Lorito et al., 2015, and references therein).

We implemented a different strategy to further reduce the number of explicit tsunami simulations and introduced a separate treatment for local and remote sources. In particular, the source scenario filtering procedure was revised to improve both the computational efficiency and the accuracy, allowing for a full scalability to the source variability of typical SPTHA (millions of scenarios located allover an entire basin). A schematic diagram of the new procedure is sketched in Fig. 1, with (right, step (3b)) or without (left, step (3a)) the separation between near- and far-field.

We still kept Filter H, but also adopted an additional filter on the occurrence probability (hereinafter "Filter P", see Fig. 1), discarding scenarios whose cumulative mean annual rate (mean of the model epistemic uncertainty) is below a fixed threshold. Filter P works as follows. Scenarios are sorted according to their mean annual rate and the rarer are~~In practice, scenarios were sorted for increasing mean annual rate and the first ones were~~ removed until the cumulated rate reaches the selected threshold. This allows to further reduce the number of required numerical simulations. On the other hand, this operation introduces a controlled downward bias on the estimated hazard, whose upper limit corresponds (on average) to the probability threshold of the filter P. This threshold can be set at a negligible level in the framework of the overall analysis and/or with respect to other uncertainties. In addition, it can be empirically checked to which extent this affects the results by analyzing the offshore hazard curves at the control points. This check was quantitatively done by computing the maximum deviation between the mean hazard curves at each control point before and after Filter P was applied. We also notice that, as reported in Fig. 1, Filter P was always applied after Filter H due to strategical reasons of optimization: in fact, the cumulate rate curve is lowered by the removal of small events (i.e., producing small H_{max}), which are typically featured by high occurrence probability. As a consequence, a greater number of scenarios can be removed before reaching the imposed threshold, making Filter P more efficient.

Also the cluster analysis stage was modified. Firstly, we used a different algorithm, as the large number of source scenarios, due to a realistic fault variability distribution, in some cases can make the HCA a computationally unaffordable task. We implemented the more efficient $k-medoids$ clustering procedure (Kaufman and Rousseeuw, 2009; Park and Jun, 2009), based on the minimization of the sum of the intra-cluster distances, that is the distances between each element of a cluster and the cluster centroid. Strong constraints on the distances result in a more accurate partitioning, in terms of similarity among the elements of each cluster, but lead to a great number of clusters. Instead, larger ranges of acceptability increase the efficiency of the algorithm, in terms of number of resulting clusters, to the detriment of the accuracy. ~~Moreover,~~ The cluster analysis was performed separately for groups of scenarios with similar mean $< H_{max} >$ along the profile, instead of grouping scenarios per earthquake magnitude classes. This makes the partitioning more efficient, as the earthquake magnitude can not be considered the only parameter controlling the tsunami intensity, as it was for the limited set of sources adopted by Lorito et al. (2015). The cluster distance was measured by the eq. 1~~same cost function implemented by Lorito et al. (2015)~~ , but we updated the stopping criterion, which is now related to the maximum allowed intra-cluster variance, rather than being a blind optimization of the number of clusters. More specifically, to control the dispersion within each cluster, we set a threshold for the maximum allowed squared Euclidean distance. This threshold was empirically fixed by comparing the offshore hazard curves before and after the analysis and assuming an acceptable range of variability, in analogy with the approach used for Filter P.

Finally, and probably most importantly, in order to deal more properly with the contribution from local sources, we implemented two independent filtering schemes for distant and local sources. Indeed, a special treatment for near-field sources is needed, as the coseismic deformation can modify the actual local tsunami intensity at the nearby coast, due to coastal uplift or subsidence. As a consequence, the offshore tsunami amplitude profiles generated by such events may fail in being representative of the coastal inundation, ~~as assumed by Lorito et al. (2015)~~, and a separate modeling is required, using the coseismic deformation~~displacement~~ as the metric for source proximity in the cluster analysis (details below). This issue was somehow hidden in Lorito et al. (2015), ~~again~~ due to the relatively small aleatory variability they considered, being the source either in the far- or near-field, depending on the target site, but never mixed together. In addition, this separation may favor some refinement of the near-field source discretization and modeling, such as a denser sampling of geometrical parameters and/or the introduction of heterogeneous slip distributions.

For testing the proposed method, we replaced step (3) either with step (3a) or step (3b), as displayed in Fig. 1. The workflow of step (3a) is substantially equivalent to the original procedure by Lorito et al. (2015), improved by ~~all~~ the afore mentioned changes related to the algorithm optimization, whereas~~except~~ the separate treatment of near- and far-field sources~~, which~~ is included in step (3b). Step (3a) is then used in this study as a term of comparison for the new scheme.

In step (3a), three sequential tasks were performed, namely Filter H, Filter P and the cluster analysis based on the offshore tsunami amplitudes.

In step (3b), local and distant sources were firstly detected, based on the coseismic deformation produced by the earthquake near and on the target coast. The procedure was then split into two parallel paths, which need to be merged at the end when evaluating SPTHA (Fig. 1). As far as the far-field scenarios are concerned, the same workflow as step (3a) was followed. Near-field scenarios, which in principle should be individually modeled, were also filtered in order to reduce the number of explicit inundation simulations: this of course introduces a new approximation, which however is better than aggregating local and remote scenarios on the basis of the offshore tsunami amplitudes. Filter H was applied as well, but choosing a smaller threshold value: a more conservative approach is indeed recommended at this stage, as offshore values could be strongly misleading when significant coastal coseismic deformation ~~of the coast~~ occurs. Then, Filter P was employed and finally a cluster analysis was performed, by comparing the coseismic ~~vertical~~ deformations, instead of the (unrepresentative) offshore tsunami amplitudes. For each local source, the vertical component of the coseismic displacement was calculated on a 2D grid centered around the fault and having size equal to three times the fault length. Then, the cluster analysis was carried out, separately for each magnitude, by comparing the coseismic fields point-to-point within~~at each point of~~ the ~~2D~~ grid. In this case, the cluster analysis is based on the squared Euclidean distance, instead of the cost function; also~~, while~~ the stopping criterion is evaluated through~~on~~ the Euclidean distance, since the coseismic field can take both positive and negative values.

The selected earthquake scenarios from step (3a) or from the two branches (near- and far-field) of step (3b) were then used for high-resolution inundation simulations and combined together in step (4) when evaluating SPTHA. A practical example of the whole procedure is illustrated in the next section.

4 The Milazzo oil refinery (Sicily, Italy) use-case

The described procedure was applied to a test site, Milazzo, located on the north eastern coast of Sicily (Italy), within the Mediterranean Sea. The site houses an oil refinery, one of the non nuclear critical infrastructures selected as case study in the framework of the EU project STREST (http://www.strest-eu.org/).

Due to the illustrative purposes of the present work, some strong assumptions were imposed during the filtering procedure to drastically reduce the number of required explicit numerical simulations~~for the sake of simplicity~~. The tuning of the filtering thresholds is not the objective of the present work; in fact, the application is aimed to highlight that inaccurate (biased) evaluation of site-specific tsunami hazard would be obtained if scenarios located in the near-field of the target area are not properly taken into account, irrespectively of the completeness and consequent complexity of the hazard assessment. However, more sanity and sensitivity tests for a finer tuning of thresholds and modeling would be mandatory in case of a real application. For example, the modeling of near-field scenarios is expected to be dependent on the source parameters, especially concerning the heterogeneous slip distribution on the fault plane (e.g., Geist and Oglesby, 2014), which was not included here. Hence~~Therefore~~, the computational effort of a real assessment, including a wider source variability and more conservative thresholds, is expected to be more complicated and computationally demanding than this case-study.

Regarding step (1), the adopted seismicity model was previously developed in the framework of the EU project ASTARTE (http://www.astarte-project.eu/). This model extends the method applied to the Ionian Sea in Selva et al. (2016) to the entire

Mediterranean Sea, including the subduction interfaces of the Calabrian and Hellenic Arcs as well as crustal seismicity in the whole basin (see Fig. 2a). On subduction zones, events of different magnitude and positions on the whole interface are allowed, disregarding the geometry uncertainty of the slab; conversely, crustal seismicity is allowed to occur with any meaningful geometry and mechanism in the whole seismogenic volume at different magnitude and depths. The complete set of sources retrieved from step (1) contains about 40 millions of elements, among which 1,701,341 scenarios actually affect the target site ($H_{max} > 0.05m$ offshore Milazzo). Although relatively simplified, the source model includes also epistemic uncertainties on many source parameters such as the seismic rates, the shape of the magnitude-frequency distribution, and the seismogenic depth interval for the two subduction zones.

Tsunami amplitudes (step (2)) were computed on a control profile made of 11 points offshore the Milazzo target area (on the $50m$ isobath), as reported in Fig. 2A. To save computational time, scenarios from step (1) were not individually simulated, but were obtained by linear combination of pre-calculated tsunami waveforms produced by Gaussian-shaped unitary sources (Molinari et al., 2016). The Gaussian propagation has been modeled by the Tsunami-HySEA code, a non-linear hydrostatic shallow-water multi-GPU code based on a mixed finite difference/finite volume method (de la Asunción et al., 2013; Macías et al., 2016, 2017).

Step (3) was addressed by independently performing the two branches (3a) and (3b), as discussed in the previous section, and then comparing results to assess the importance of the separate treatment of the near-field sources.

In step (3a), thresholds were fixed at $1m$ for Filter H and $10^{-5}yr^{-1}$ for Filter P. This resulted in discarding scenarios with individual mean annual rate below $\sim 10^{-9}yr^{-1}$, causing a maximum bias on the offshore mean hazard curves of about 10% in the considered range of tsunami intensities, with respect to the curves obtained without Filter P~~, as explained before in Section 3~~. At the end of the filtering procedure, imposing a threshold equal to 0.2 on the intra-cluster variance, we obtained 776 clusters, each associated to a representative scenario. That is~~Namely~~, we had a reduction ~~even~~ above 99%. Figure S1 of the Supplementary Material shows the comparison among the mean offshore hazard curves at the 11 control points, as well as among some quantiles of the epistemic uncertainty, for the filtered and original set of scenarios.

It is worth stressing that the efficiency of the filters is here artificially enhanced by the imposed high thresholds, especially as far as the Filter H is concerned. While $1m$ is not an acceptable value in case of a real hazard assessment, it is suitable for illustrative purposes. In any case, this filter, independently from the chosen threshold, is not expected to affect subsequent steps of the procedure for tsunami intensities above the threshold. Conversely, we performed a sensitivity analysis on the threshold imposed on the intra-cluster variance for the cluster analysis: Fig. S2 shows the percentage differences between the offshore hazard curves computed from the complete initial set of sources and the filtered set. The red box corresponds to the chosen threshold value (0.2): it appears evident that a smaller value would have allowed a stronger constraint on the error introduced by the cluster analysis, while considerably increasing the number of resulting clusters. Vice versa, higher thresholds produce a smaller number of clusters, but fail in reproducing the hazard (error up to 40%). In case of a real hazard assessment, this analysis would help choosing an optimal threshold.

In step (3b), we considered as local scenarios, requiring a separate processing, sources generating a coseismic vertical displacement greater than or equal to $0.5m$ on a set of near-field points, that is the 11 control points on the $50m$ isobath plus

95 inland points, strategically located at the edges of the refinery storage tanks, as shown in Fig. 2B. We found 4721 scenarios in the near-field (see Fig. 2A). Afterward, for both branches we applied Filter H and P as well, using the following thresholds: for far-field scenarios, Filter H=$1m$ and Filter P=$5 \times 10^{-6} yr^{-1}$; for near-field scenarios, Filter H=$0.1m$, according to the more conservative approach described in the previous section, and Filter P=$5 \times 10^{-6} yr^{-1}$. Note that Filter P threshold was set half the value used in step (3a), in order to keep a total maximum theoretical bias on the hazard curves at $10^{-5} yr^{-1}$ (as in step (3a)), considering that Filter P is separately applied both to far- and near-field scenarios. Then, the cluster analysis was carried out on the tsunami amplitudes for far-field scenarios (using a threshold equal to 0.2 on the intra-cluster variance) and on the coseismic deformation for near-field scenarios (using a 10% threshold for the intra-cluster variance). We obtained 634 and 520 clusters for remote and local sources, respectively. Thus, the total number of representative scenarios (1154) to be explicitly modeled corresponds to a reduction above 99% of the initial set of sources.~~that is a total of 1154 scenarios to be explicitly modeled, again corresponding to a reduction above 99% of the initial set of sources.~~

Inundation simulations at step (3) have been carried out again with the Tsunami-HySEA code, exploiting the nested grid algorithm. We used 4-level nested bathymetric grids with refinement ratio equal to 4 and increasing resolution from $0.4arc-min$ ($\sim 740m$) to $0.1arc-min$ ($\sim 185m$) to $0.025arc-min$ ($\sim 46m$) to $0.00625arc-min$ ($\sim 11m$). The largest grid was obtained by resampling the SRTM15+ bathymetric model (http://topex.ucsd.edu/WWW_html/srtm30_plus.html). The finest three grids have been produced by interpolation from TINITALY (inland, Tarquini et al. (2007, 2012)) and EMODNET (offshore, http://www.emodnet-bathymetry.eu/), working on grids of $0.00625arc-min$ that have been resampled at $0.1arc-min$ and $0.025arc-min$. A picture of the telescopic nested grids is provided in Fig. S1 of the Supplementary Material. The initial conditions were differently provided for subduction and crustal seismicity. The subduction scenarios have been simulated by modeling the slab as a 3D triangular mesh honoring the interface profile and using unitary Okada sources associated to each element of the mesh (i.e., to each triangle) as Green's functions (Okada, 1985; Meade, 2007). For crustal events, the initial sea level elevation was obtained by modeling the dislocation on rectangular faults according to the Okada model. A Kajiura-like filter for the sea-bottom/water-surface transfer of the dislocation was also applied (Kajiura, 1963). For each simulation an overall length of 8 hours was fixed. The results were stored as maximum wave height (H_{max}, m) and maximum momentum flux (MF_{max}, m^3s^{-2}), at each point of the inner grid.

At step (4), SPTHA was evaluated in parallel using results both from steps (3a) and (3b), in order to compare the outcomes of the two different workflows and estimate the impact of the special treatment of near-field sources on the site-specific hazard assessment. Note that alternative models for the epistemic uncertainty were considered only at step (1), that is only as far as the probabilistic earthquake model is concerned, since the Selva et al. (2016) model was used.

Figures 3 to 5 compare the results from steps (3a) and (3b), in terms of mean hazard curves and inundation (both probability and hazard) maps for H_{max}. ~~In the Supplementary Material, analogous figures for~~ ~~MF_{max}~~ ~~are provided (Figs. S2 to S4).~~ At a first glance, differences are appreciable~~evident~~ in both the curves and the maps. It is worth noting that results at $H_{max} < 1m$ can be (negatively) biased since they are depleted from the scenarios removed by~~can not be considered meaningful, as that is the chosen threshold for~~ Filter H , both in step (3a), as clearly shown in Fig. S1, and in the far-field-branch of step (3b). Curves and maps will be described in more detail in the following.

The hazard curves in Fig. 3 (panels a) and b)) show the mean (mean of the model epistemic uncertainty) exceedance probability in $50yr$ for H_{max} (evaluated assuming a Poisson process, as in Selva et al. (2016)), plotted for each point of the finest resolution grid. Panel c) of the same figure displays the one-by-one relative differences in terms of exceedance probability (in $50yr$), as a function of H_{max}, between the step (3a) and (3b) curves at each grid point. For values of H_{max} greater than $1m$, the relative differences are systematically positive, meaning that without the correction for near-field scenarios (step (3a)), the tsunami intensity would be overestimated. We may argue that this is true in the case of this specific setting, as a lower "corrected" hazard means that the predominant effect by local sources contributing to a specific point on the hazard curve is due to the coastal uplift, which in turn decreases the tsunami hazard. For example, a cluster may mix far- and near-field sources, which could be misrepresented by one far-field source selected as cluster representative. In our case, there might be a prevalence of clusters causing coastal uplift from the near-field sources. The situation may be the opposite for a different source-target configuration, that is coastal subsidence could be predominant causing an hazard increase, which without correction would be underestimated. To confirm our inference, we performed some further testing. For each hazard intensity, and only for the mean model of the epistemic uncertainty, we computed the coseismic coastal displacement in the inner grid, averaged both over all of the scenarios and over all of the coastal points (purple line in Fig. 3c). This quantity can be regarded as the mean uplift (hereinafter MU) on a random point on the coastline. Scenarios of different types contribute to MU, both far-field scenarios, which do not alter the coastline, and near-field scenarios, which may include a mixture of sources producing both coastal subsidence and uplift. More in detail, we firstly performed, for each H_{max}, a weighted average of the coseismic displacements from each cluster centroid, with weights equal to the annual probability of the individual earthquakes. These probabilities are set to zero if the earthquake do not deform the coastline (i.e. for far-field sources) or if the generated tsunami does not exceed the given H_{max} value (i.e. that scenario does not contribute to the hazard at that point). The weighted average is then normalized to the total probability of the near- and far-field sources contributing to the tsunami hazard for that threshold. The resulting MU on each coastal point is plotted, for different values of $H_{max} \geq 1m$, in Fig. S4 of the Supplementary Material (blue lines). The displacements due to the single cluster representatives are also shown (red lines). We note that, although single scenarios produce both positive and negative coastal displacements, the predominant contribution is unveiled by the sum over the different clusters, which is definitely positive. Finally, we further averaged the resulting values along the coastline, obtaining the purple curve in Fig. 3c. We notice that the absolute MU value in meters turns out to be rather small, as a result of the average over sources that cause either uplift or subsidence, or no coastal displacement at all. Anyway, the obtained positive values indicate that the uplift of the coast is prevailing, consistently with the positive percentage differences retrieved between the two approaches for $H_{max} > 1m$. Very little differences are retrieved between the "corrected" and the "uncorrected" filtering procedures for smaller values of H_{max}, that is below the Filter H threshold.~~For small values of H_{max}, the envelope of the curves obtained from step (3b) is systematically higher than that from step (3a), with a stronger negative gradient up to $3m$. This means that the largest probabilities would be underestimated without the correction for the near-field sources. For values greater than $3m$, the differences between the envelopes of the families of curves are less pronounced and the maximum hazard is slightly - although systematically - lower for step (3b). A more complex pattern emerges when analyzing the one-by-one relative differences in terms of exceedance probability (in $50yr$), as a function of H_{max}, between the~~

~~step (3a) and (3b) curves at each grid point (panel c) of the same figure). Note that a positive difference means that step (3a) overestimates the probability for a given H_{max} value. For values below $3m$, the median confirms the underestimation without the correction, although individual grid points are dispersed and assume both positive and negative values. For values greater than $3m$, there is a definite overestimation without the correction (step (3a)), both as far as the median and the individual points are concerned.~~

Finally, in Fig. 3d the relative differences are also shown in terms of H_{max} as a function of exceedance probability (in $50yr$). In the low probability region, typically~~supposedly~~ corresponding to high H_{max}, the overestimation by step (3a) is confirmed; conversely, for exceedance probability greater than $\sim 10^{-4}$, which is likely to correspond to small H_{max}, a greater dispersion with both positive and negative values is observed~~the differences are almost all negative. In other words, in this range, for a given average return period (ARP), the predicted H_{max} turns out to be greater when step (3b) is used.~~

Probability and hazard inundation maps can be achieved by vertically and horizontally cutting the hazard curves at chosen fixed values, in order to give a geographical representation of results. As each hazard curve corresponds to a grid point, the probability maps are obtained by plotting on a map all the probability values for a fixed value of the intensity metric. Instead, in the hazard maps the intensity values are plotted for a fixed exceedance probability, corresponding to a given ARP. In Fig. 4 we computed the exceedance probability maps for $H_{max} = 2m$ and $H_{max} = 3m$, while in Fig. 5 we extracted the hazard maps for $ARP = 2 \times 10^5 yr$ and $ARP = 3 \times 10^5 yr$ (corresponding to an exceedance probability in $50yr$ equal to 2.5×10^{-4} and 1.7×10^{-4}, respectively).

For the selected values, the maps confirm what we already discussed about the curves: from the probability maps ,~~show~~ mostly positive relative differences both inland and offshore are inferred, as shown in panels (c) and (f) of Fig. 4, even larger than 50%; these differences are positive in a larger number of points~~, even offshore,~~ for the higher intensity, consistently with Fig. 3c. We recall that positive differences mean that the "uncorrected" procedure (step (3a)) actually overestimates the tsunami hazard at the target site. Negative inland values are also observed for $H_{max} = 2m$, but they occur for very low probability values and should not be further investigated. We also notice that the area inundated with a non negligible probability decreases in size with increasing the H_{max} value, as expected. ~~On the other hand,~~ In the hazard maps (Fig. 5) a complex pattern is revealed when inspecting the relative differences (panels (c) and (f)), as both positive and negative values are retrieved. This happens because ~~differences are negative, namely H_{max} retrieved from step (3b) is smaller than from step (3a), as~~ the analyzed ARPs lie in the low intensity range. The inundated area, as opposite to the previous case, is consistently more extended for larger ARPS.~~We also notice that the inundated area decreases with increasing the H_{max} value, as expected.~~

Further details about the comparison can be found by analyzing the curves and the maps for MF_{max}~~the maximum momentum flux~~ reported in Figs. S5 to S7 of the Supplementary Material . We just note that ~~the envelope of the hazard curves obtained from step (3b) is definitely above the curves from step (3a) in the entire range of MF_{max} (see Fig. S5); moreover~~, when the correction for near-field is taken into account, the inundation maps highlight an enhanced current vorticity near the docks (Fig. S6(b,e) and S7(b,e)), which is a known effect due to the flow separation at the tip of a breakwater (Borrero et al., 2015). As the probability and hazard maps aggregate several different sources, the hazard integral may tend to average and cancel out different source effects, while enhancing local propagation features. The presence of such persistent physically meaningful effects only in the maps retrieved using step (3b) confirms the importance of the special treatment. In other words, the blind cluster analysis (step (3a)), exclusively based on the offshore tsunami amplitudes, likely produced a non-representative selection of the important scenarios, as it could aggregate or even remove important local scenarios.

5 Conclusions

We proposed a computationally efficient approach to achieve robust assessment of site-specific SPTHA, developing an improved version of the method by Lorito et al. (2015) and Selva et al. (2016).

The procedure is based on 4 steps, which can be summarized~~resumed~~ as follows:(1) the definition of the ~~whole~~ set of earthquake scenarios ~~affecting the target site~~ and their mean annual rates, ~~fully~~ exploring the source aleatory uncertainty; (2) the computation of tsunami propagation up to an offshore isobath; (3) the implementation of a filtering procedure to select relevant scenarios for the target site, which are then explicitly modeled; (4) the assessment of local SPTHA through an ensemble modeling approach, to jointly quantify aleatory and epistemic uncertainty, stemming from alternative models for steps (1)-(3).

In the present work we ~~mainly~~ focused on step (3), modifying the filtering procedure to enhance the computational efficiency and introducing a separate treatment for sources located in the near-field, to take into account the effect of the coseismic deformation on the tsunami intensity. To this aim, we implemented a new procedure including a correction for near-field and some numerical improvements. We benchmarked the new approach against an algorithm essentially equivalent to the original method by Lorito et al. (2015). The correction~~This~~ is crucial as the latter~~original method~~ is based on the assumption that offshore tsunami profile is representative of the inundation at the nearby coast, which might be~~is actually~~ true if a coseismic deformation of the coast is not involved; otherwise seafloor uplift or subsidence make the assumption invalid ~~as the tsunami intensity is not predictable from offshore wave amplitudes~~. Consequently, local and remote sources must be separately treated by means of~~and, to ensure a feasible computational effort by reducing the number of explicit inundation simulations,~~ different filtering procedures~~ must be employed in the far- and near-field~~. This may also allow for a specific and more detailed parameterization of the near-field sources, to which the local hazard is known to be more sensitive.

We tested the procedure investigating a case study, i.e. Milazzo (Sicily)~~, a test-site selected within the STREST project (http://www.strest-eu.org/)~~. The work has only illustrative purposes and is not~~has not to be~~ intended as a real hazard assessment at that site, due to some simplifications in the adopted~~implemented~~ model. ~~The results highlight that near-field sources play a fundamental role, as expected, and confirm that they must be specifically dealt with when evaluating site-specific SPTHA. Moreover,~~

The new implemented filtering procedure allows for a consistent reduction of the number of tsunami inundation simulations and therefore of the computational cost of the analysis. It is worth stressing that in this specific application the computational efficiency was artificially enhanced by limiting the source variability as well as by imposing high filter thresholds. In fact, a real assessment is expected to deal with a greater number of scenarios, provided that a finer tuning of the threshold values is carried out. This may in particular affect the computational cost related to the analysis of the near-field sources, for example when using stochastic slip distributions.

~~A quantitative evaluation of the coseismic effect on the tsunami hazard is not straightforward, as it depends on which sources contribute to each point of the hazard curves and their relative position with respect to the target site. As a consequence, coastal deformation can not be deduced as a whole by comparing the hazard curves obtained with and without the differentiation between far- and near-field. Here,~~ The most striking result is that the separate treatment of near-field sources provides significantly different and physically more consistent results with respect to the "uncorrected" procedure, showing that near-field sources must be specifically dealt with when evaluating site-specific SPTHA. We recall that the two approaches (with or without the correction for near-field) only differ in the way local sources are treated. Hence, the different results do not depend on the specific filtering thresholds but just on the coseismic deformation induced by local sources, which, if properly accounted for, modifies the effective tsunami hazard. Actually, for the specific configuration of this use-case, our findings reveal that not considering an appropriate correction for near-field would lead to overestimate the tsunami hazard for H_{max} greater than $1m$, and this overestimation is correlated to dominant coastal uplift.~~for relatively large intensities the tsunami hazard would be overestimated if local sources were not explicitly modeled, suggesting a coastal uplift caused by the near coseismic field. For relatively low intensities, the hazard curves indicate a more complex pattern and the overall maxima would be instead underestimated without the correction for near-field.~~ However, different cases in terms of over- and under-estimation may occur at different sites, depending on the relative source-site configuration. We also observe that Milazzo is located in an area featuring relatively low near-field tsunamigenic seismicity with respect to other areas in the Mediterranean sea. Nevertheless, the method turns out to be sensitive even to relatively low displacements and allows to detect and remove significant biases from near-field sources.

The proposed method is suitable to be applied to operational assessments, also for improving local (multi-hazard) risk analyses (e.g. Goda and De Risi, 2018). We stress again that the approach developed here allows to consider a very high number of tsunami scenarios, which is necessary to sufficiently explore the natural variability of the tsunami sources and the eventual alternative models needed for quantifying the epistemic uncertainty.

Future work will be devoted to use the procedure to perform real local hazard assessment, exploiting the regional hazard retrieved from the TSUMAPS-NEAM project.

Competing interests. The authors declare that they have no conflict of interest.

Acknowledgements. The authors want to thank the EDANYA Research Group at University of Malaga for providing the Tsunami-HySEA code for tsunami simulations. We acknowledge useful discussions with William Power and Gareth Davies during the early stages of this work. We also acknowledge constructive comments by three anonymous referees, which allowed a significant improvement of this paper. The work was partially funded by INGV–DPC Agreement (Annex B2) and by the STREST project, EC's Seventh Framework Programme [FP7/2007-2013], grant agreement n. 603389. All of the figures have been created using either MATLAB (www.mathworks.com) and Generic Mapping Tools (http://gmt.soest.hawaii.edu).

References

Basili, R., Tiberti, M. M., Kastelic, V., Romano, F., Piatanesi, A., Selva, J., and Lorito, S.: Integrating geologic fault data into tsunami hazard studies, Nat. Hazards Earth Syst. Sci., 13, 1025–1050, https://doi.org/10.5194/nhess-13-1025-2013, 2013.

Bazzurro, P. and Cornell, C.: Disaggregation of seismic hazard, Bull. seism. Soc. Am., 89, 501–520, 1999.

Borrero, J. C., Lynett, P. J., and Kalligeris, N.: Tsunami currents in ports, Philosophical Transactions of the Royal Society of London A: Mathematical, Physical and Engineering Sciences, 373, https://doi.org/10.1098/rsta.2014.0372, 2015.

Brizuela, B., Armigliato, A., and Tinti, S.: Assessment of tsunami hazards for the Central American Pacific coast from southern Mexico to northern Peru, Natural Hazards and Earth System Sciences, 14, 1889–1903, https://doi.org/10.5194/nhess-14-1889-2014, 2014.

Burbidge, D., Cummins, P. R., Mleczko, R., and Thio, H. K.: A Probabilistic Tsunami Hazard Assessment for Western Australia, Pure Appl. Geophys., 165, 2059–2088, https://doi.org/10.1007/s00024-008-0421-x, 2008.

Chock, G., Yu, G., Thio, H. K., and Lynett, P. J.: Target Structural Reliability Analysis for Tsunami Hydrodynamic Loads of the ASCE 7 Standard, Journal of Structural Engineering, 142, https://doi.org/10.1061/(ASCE)ST.1943-541X.0001499, 2016.

Davies, G., Horspool, N., and Miller, V.: Tsunami inundation from heterogeneous earthquake slip distributions: Evaluation of synthetic source models, J. Geophys. Res.: Solid Earth, 120, 6431–6451, https://doi.org/10.1002/2015JB012272, 2015.

Davies, G., Griffin, J., Løvholt, F., Glimsdal, S., Harbitz, C., Thio, H. K., Lorito, S., Basili, R., Selva, J., Geist, E., and Baptista, M. A.: A global probabilistic tsunami hazard assessment from earthquake sources, Geological Society, London, Special Publications, 456, https://doi.org/10.1144/SP456.5, 2017.

de la Asunción, M., Castro, M. J., Fernández-Nieto, E., Mantas, J. M., Acosta, S. O., and González-Vida, J. M.: Efficient GPU implementation of a two waves TVD-WAF method for the two-dimensional one layer shallow water system on structured meshes, Computers & Fluids, 80, 441 – 452, https://doi.org/https://doi.org/10.1016/j.compfluid.2012.01.012, http://www.sciencedirect.com/science/article/pii/S0045793012000217, selected contributions of the 23rd International Conference on Parallel Fluid Dynamics ParCFD2011, 2013.

Gailler, A., Calais, E., Hébert, H., Roy, C., and Okal, E.: Tsunami scenarios and hazard assessment along the northern coast of Haiti, Geophysical Journal International, 203, 2287–2302, https://doi.org/10.1093/gji/ggv428, 2015.

Geist, E. L.: Complex earthquake rupture and local tsunamis, Journal of Geophysical Research: Solid Earth, 107, ESE 2–1–ESE 2–15, https://doi.org/10.1029/2000JB000139, 2002.

Geist, E. L. and Lynett, P. J.: Source Processes for the Probabilistic Assessment of Tsunami Hazards, Oceanography, 27, https://doi.org/10.5670/oceanog.2014.43, 2014.

Geist, E. L. and Oglesby, D. D.: Tsunamis: Stochastic Models of Occurrence and Generation Mechanisms, pp. 1–29, Springer New York, New York, NY, https://doi.org/10.1007/978-3-642-27737-5_595-1, 2014.

Geist, E. L. and Parsons, T.: Probabilistic analysis of tsunami hazards, Nat. Hazards, 37, 277–314, https://doi.org/10.1007/s11069-005-4646-z, 2006.

Goda, K. and De Risi, R.: Multi-hazard loss estimation for shaking and tsunami using stochastic rupture sources, International Journal of Disaster Risk Reduction, 28, 539 – 554, https://doi.org/10.1016/j.ijdrr.2018.01.002, 2018.

González, F. I., Geist, E. L., Jaffe, B., Kanoglu, U., Mofjeld, H., Synolakis, C. E., Titov, V. V., Areas, D., Bellomo, D., Carlton, D., Horning, T., Johnson, J., Newman, J., Parsons, T., Peters, R., Peterson, C., Priest, G., Venturato, A., Weber, J., Wong, F., and Yalciner, A.: Probabilistic tsunami hazard assessment at Seaside, Oregon, for near-and far-field seismic sources, J. Geophys. Res.: Solid Earth, 114, https://doi.org/10.1029/2008JC005132, 2009.

Grezio, A., Babeyko, A., Baptista, M. A., Behrens, J., Costa, A., Davies, G., Geist, E. L., Glimsdal, S., González, F. I., Griffin, J., Harbitz, C. B., LeVeque, R. J., Lorito, S., Løvholt, F., Omira, R., Mueller, C., Paris, R., Parsons, T., Polet, J., Power, W., Selva, J., Sørensen, M. B., and Thio, H. K.: Probabilistic Tsunami Hazard Analysis (PTHA): multiple sources and global applications, Rev. of Geophys., https://doi.org/10.1002/2017RG000579, 2017.

Griffin, J. D., Pranantyo, I. R., Kongko, W., Haunan, A., Robiana, R., Miller, V., Davies, G., Horspool, N., Maemunah, I., Widjaja, W. B., Natawidjaja, D. H., and Latief, H.: Assessing tsunami hazard using heterogeneous slip models in the Mentawai Islands, Indonesia, Geological Society of London Special Publications, 441, 47–70, https://doi.org/10.1144/SP441.3, 2017.

Gusman, A. R., Tanioka, Y., MacInnes, B. T., and Tsushima, H.: A methodology for near-field tsunami inundation forecasting: Application to the 2011 Tohoku tsunami, Journal of Geophysical Research: Solid Earth, 119, 8186–8206, https://doi.org/10.1002/2014JB010958, 2014.

Harbitz, C., Glimsdal, S., Bazin, S., Zamora, N., Løvholt, F., Bungum, H., Smebye, H., Gauer, P., and Kjekstad, O.: Tsunami hazard in the Caribbean: Regional exposure derived from credible worst case scenarios, Continental Shelf Research, 38, 1 – 23, https://doi.org/https://doi.org/10.1016/j.csr.2012.02.006, http://www.sciencedirect.com/science/article/pii/S0278434312000349, 2012.

Hoechner, A., Babeyko, A. Y., and Zamora, N.: Probabilistic tsunami hazard assessment for the Makran region with focus on maximum magnitude assumption, Nat. Hazards Earth Syst. Sci., 16, 1339–1350, https://doi.org/10.5194/nhess-16-1339-2016, 2016.

Horspool, N., Pranantyo, I., Griffin, J., Latief, H., Natawidjaja, D. H., Kongko, W., Cipta, A., Bustaman, B., Anugrah, S. D., and Thio, H. K.: A probabilistic tsunami hazard assessment for Indonesia, Nat. Hazards Earth Syst. Sci., 14, 3105–3122, https://doi.org/10.5194/nhess-14-3105-2014, https://www.nat-hazards-erth-syst-sci.net/14/3105/2014/, 2014.

Kajiura, K.: The leading wave of a tsunami, Bull. Earthquake Res. Inst., 41, 535–571, 1963.

Kaufman, L. and Rousseeuw, P. J.: Finding Groups in Data: An Introduction to Cluster Analysis, Hoboken, New Jersey: John Wiley & Sons, Inc., 2009.

Lay, T.: The surge of great earthquakes from 2004 to 2014, Earth Planet. Sc. Lett., 409, 133–146, https://doi.org/10.1016/j.epsl.2014.10.047, 2015.

LeVeque, R., Waagan, K., González, F., Rim, D., and Lin, G.: Generating random earthquake events for probabilistic tsunami hazard assessment, Pure Appl. Geophys., 173, 3671–3692, https://doi.org/10.1007/s00024-016-1357-1, 2016.

Li, L., Switzer, A. D., Chan, C.-H., Wang, Y., Weiss, R., and Qiu, Q.: How heterogeneous coseismic slip affects regional probabilistic tsunami hazard assessment: A case study in the South China Sea, J. Geophys. Res.: Solid Earth, 121, 6250–6272, https://doi.org/10.1002/2016JB013111, 2016.

Lin, I. and Tung, C.: A preliminary investigation of tsunami hazard, Bull. seism. Soc. Am., 72, 2323–2337, 1982.

Lorito, S., Tiberti, M. M., Basili, R., Piatanesi, A., and Valensise, G.: Earthquake-generated tsunamis in the Mediterranean Sea: Scenarios of potential threats to Southern Italy, J. Geophys. Res.: Solid Earth, 113, B01 301, https://doi.org/10.1029/2007JB004943, 2008.

Lorito, S., Piatanesi, A., Cannelli, V., Romano, F., and Melini, D.: Kinematics and source zone properties of the 2004 Sumatra-Andaman earthquake and tsunami: Nonlinear joint inversion of tide gauge, satellite altimetry, and GPS data, J. Geophys. Res.: Solid Earth, 115, https://doi.org/10.1029/2008JB005974, 2010.

Lorito, S., Selva, J., Basili, R., Romano, F., Tiberti, M. M., and Piatanesi, A.: Probabilistic Hazard for Seismically-Induced Tsunamis: Accuracy and Feasibility of Inundation Maps, Geophys. J. Int., 200, 574–588, https://doi.org/10.1093/gji/ggu408, 2015.

Lorito, S., Romano, F., and Lay, T.: Tsunamigenic Major and Great Earthquakes (2004–2013): Source Processes Inverted from Seismic, Geodetic, and Sea-Level Data, in: Encyclopedia of Complexity and Systems Science, edited by Meyers, R. A., pp. 1–52, Springer Berlin Heidelberg, Berlin, Heidelberg, https://doi.org/10.1007/978-3-642-27737-5_641-1, 2016.

Løvholt, F., Bungum, H., Harbitz, C. B., Glimsdal, S., Lindholm, C. D., and Pedersen, G.: Earthquake related tsunami hazard along the western coast of Thailand, Natural Hazards and Earth System Sciences, 6, 979–997, https://doi.org/10.5194/nhess-6-979-2006, 2006.

Løvholt, F., Glimsdal, S., Harbitz, C. B., Zamora, N., Nadim, F., Peduzzi, P., Dao, H., and Smebye, H.: Tsunami hazard and exposure on the global scale, Earth-Science Reviews, 110, 58–73, https://doi.org/10.1016/j.earscirev.2011.10.002, 2012a.

Løvholt, F., Pedersen, G., Bazin, S., Kühn, D., Bredesen, R. E., and C., H.: Stochastic analysis of tsunami runup due to heterogeneous coseismic slip and dispersion, Journal of Geophysical Research: Oceans, 117, https://doi.org/10.1029/2011JC007616, 2012b.

Løvholt, F., Davies, G., Griffin, J., Lorito, S., Volpe, M., Romano, F., Galvez, M. S., Geist, E., Ross, S., Ayrebe, I. A., Fraser, S., Thio, H. K., Canals, M., Gonzalez, F., Polet, J., Mokhtari, M., Kanoglu, U., Paris, R., Andrade, C., Baptista, M. A., Latief, H., and Papadopoulos, G.: Tsunami Hazard and Risk Assessment, in: Words into Action guidelines: National disaster risk assessment, Hazard Specific Risk Assessment, chap. 2, United Nations Office for Disaster Risk Reduction (UNISDR), https://doi.org/10.1007/978-3-642-27737-5_641-1, 2017.

Lynett, P., Wei, Y., and Arcas, D.: Tsunami Hazard Assessment: Best Modeling Practices and State-of-the-Art Technology, Nureg/cr-7223, U.S.NRC, 2016.

Macías, J., Mercado, A., Gonzalez-Vida, J. M., Ortega, S., and Castro, M.: Comparison and Computational Performance of Tsunami-HySEA and MOST Models for LANTEX 2013 Scenario: Impact Assessment on Puerto Rico Coasts, Pure Appl. Geophys., pp. 1–25, https://doi.org/10.1007/s00024-016-1387-8, 2016.

Macías, J., Castro, M. J., Ortega, S., Escalante, C., and González-Vida, J. M.: Performance Benchmarking of Tsunami-HySEA Model for NTHMP's Inundation Mapping Activities, Pure Appl. Geophys., 174, 3147–3183, https://doi.org/10.1007/s00024-017-1583-1, 2017.

Marzocchi, W., Taroni, M., and Selva, J.: Accounting for epistemic uncertainty in PSHA: Logic Tree and ensemble modeling, Bull. seism. Soc. Am., 105, 2151–2159, https://doi.org/10.1785/0120140131, 2015.

Meade, B. J.: Algorithms for the calculation of exact displacements, strains, and stresses for triangular dislocation elements in a uniform elastic half space, Computers & Geosciences, 33, 1064–1075, https://doi.org/10.1016/j.cageo.2006.12.003, 2007.

Molinari, I., Tonini, R., Piatanesi, A., Lorito, S., Romano, F., Melini, D., Vida, J. G., Macias, J., Castro, M., and de la Asuncion, M.: Fast evaluation of tsunami scenarios: uncertainty assessment for a Mediterranean Sea database, Nat. Hazards Earth Syst. Sci., 16, 2593–2602, https://doi.org/10.5194/nhess-16-2593-2016, 2016.

Mueller, C., Power, W., Fraser, S., and Wang, X.: Effects of rupture complexity on local tsunami inundation: Implications for probabilistic tsunami hazard assessment by example, J. Geophys. Res.: Solid Earth, 120, 488–502, https://doi.org/10.1002/2014JB011301, 2014.

Murphy, S., Scala, A., Herrero, A., Lorito, S., Festa, G., Trasatti, E., Tonini, R., Romano, F., Molinari, I., and Nielsen, S.: Shallow slip amplification and enhanced tsunami hazard unravelled by dynamic simulations of mega-thrust earthquakes, Sci. Rep., 6, https://doi.org/10.1038/srep35007, 2016.

Okada, Y.: Surface deformation due to shear and tensile faults in a half-space, Bull. seism. Soc. Am., 75, 1135–1154, 1985.

Park, H. S. and Jun, C. H.: A simple and fast algorithm for K-medoids clustering, Expert Systems with Applications, 36, 3336–3341, https://doi.org/10.1016/j.eswa.2008.01.039, 2009.

Power, W., Wang, X., Wallace, L., Clark, K., and Mueller, C.: The New Zealand Probabilistic Tsunami Hazard Model: development and implementation of a methodology for estimating tsunami hazard nationwide, Geological Society, London, Special Publications, 456, https://doi.org/10.1144/SP456.6, 2017.

Rikitake, B. T. and Aida, I.: Tsunami hazard probability in Japan, Bull. seism. Soc. Am., 78, 126–1278, 1988.

Romano, F., Piatanesi, A., Lorito, S., and Hirata, K.: Slip distribution of the 2003 Tokachi-oki M-w 8.1 earthquake from joint inversion of tsunami waveforms and geodetic data, J. Geophys. Res.: Solid Earth, 115, https://doi.org/10.1029/2009JB006665, 2010.

Satake, K., Fujii, Y., Harada, T., and Namegaya, Y.: Time and Space Distribution of Coseismic Slip of the 2011 Tohoku Earthquake as Inferred from Tsunami Waveform DataTime and Space Distribution of Coseismic Slip of the 2011 Tohoku Earthquake, Bulletin of the Seismological Society of America, 103, 1473, https://doi.org/10.1785/0120120122, 2013.

Selva, J., Tonini, R., Molinari, I., Tiberti, M. M., Romano, F., Grezio, A., Melini, D., Piatanesi, A., Basili, R., and Lorito, S.: Quantification of source uncertainties in Seismic Probabilistic Tsunami Hazard Analysis (SPTHA), Geophys. J. Int., 205, 1780–1803, https://doi.org/10.1093/gji/ggw107, 2016.

Sepúlveda, I., Liu, P. L., Grigoriu, M., and Pritchard, M.: Tsunami hazard assessments with consideration of uncertain earthquake slip distribution and location, J. Geophys. Res.: Solid Earth, 122, 7252–7271, https://doi.org/10.1002/2017JB014430, 2017.

Synolakis, C. and Kânoğlu, U.: The Fukushima accident was preventable, Philosophical Transactions of the Royal Society of London A: Mathematical, Physical and Engineering Sciences, 373, https://doi.org/10.1098/rsta.2014.0379, 2015.

Tarquini, S., Isola, I., Favalli, M., Mazzarini, F., Bisson, M., Pareschi, M. T., and Boschi, E.: TINITALY/01: a new Triangular Irregular Network of Italy, Annals of Geophysics, 50, 407–425, https://doi.org/10.4401/ag-4424, 2007.

Tarquini, S., Vinci, S., Favalli, M., Doumaz, F., Fornaciai, A., and Nannipieri, L.: Release of a 10-m-resolution DEM for the Italian territory: Comparison with global-coverage DEMs and anaglyph-mode exploration via the web, Computers & Geosciences, 38, 168 – 170, https://doi.org/https://doi.org/10.1016/j.cageo.2011.04.018, 2012.

Thio, H. K., Somerville, P. G., and Polet, J.: Probabilistic Tsunami Hazard Analysis, Pacific Earthquake Engineering Research Center, PEER Report 2010/108, 2010.

Tinti, S. and Armigliato, A.: The use of scenarios to evaluate tsunami impact in southern Italy, Mar. Geol., 199, 221–243, 2003.

Tonini, R., Armigliato, A., Pagnoni, G., Zaniboni, F., and Tinti, S.: Tsunami hazard for the city of Catania, eastern Sicily, Italy, assessed by means of Worst-case Credible Tsunami Scenario Analysis (WCTSA), Natural Hazards and Earth System Sciences, 11, 1217–1232, https://doi.org/10.5194/nhess-11-1217-2011, 2011.

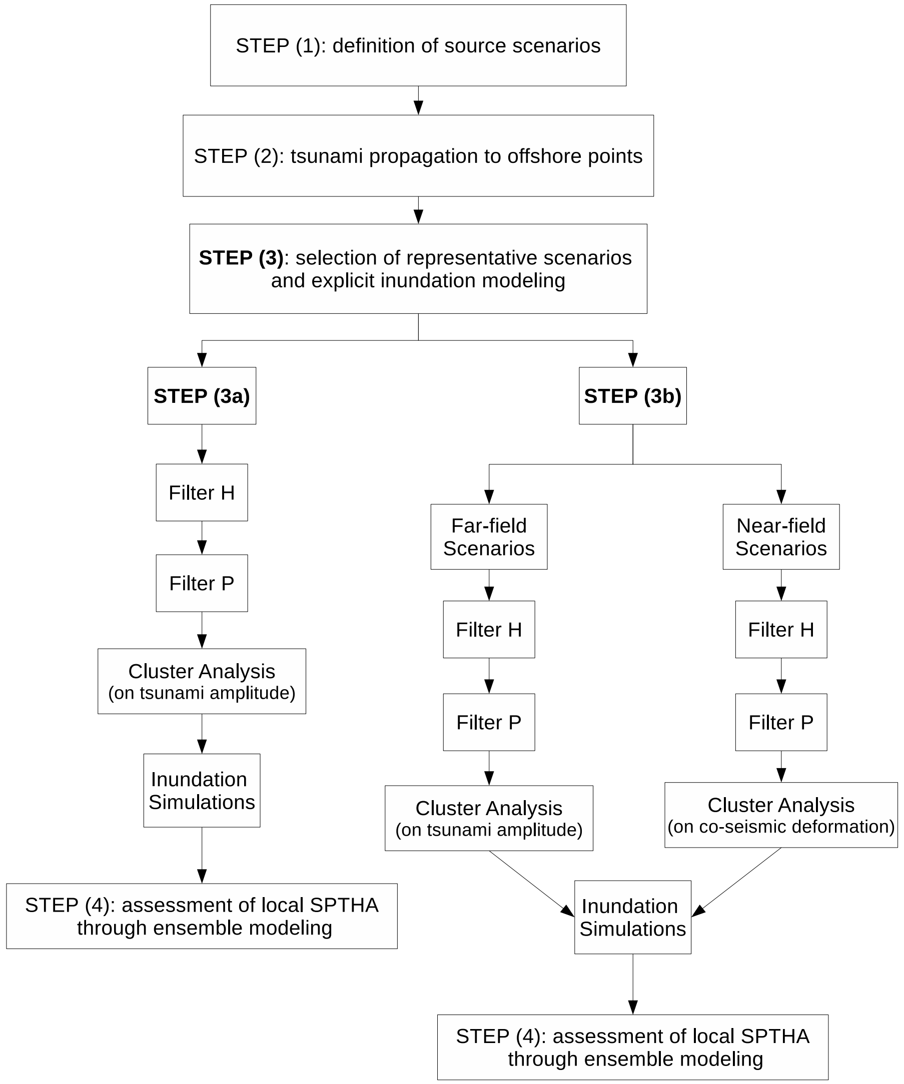

Figure 1. Schematic diagram of the computational procedure to evaluate site-specific SPTHA, with special attention to step (3) (see text).

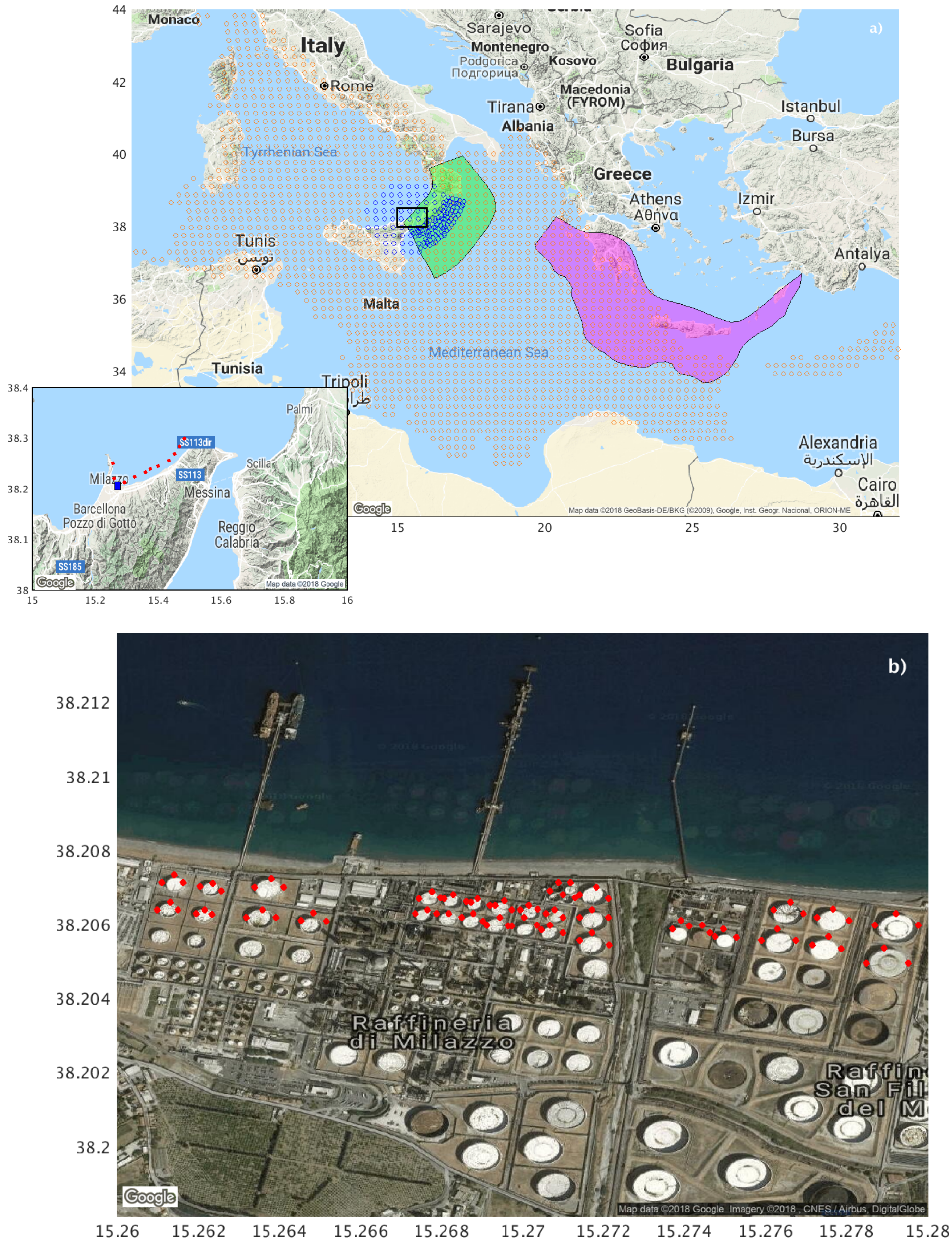

Figure 2. a) Map of the whole simulation domain used for the application at the target site Milazzo (Sicily, Italy). The orange circles are the geometrical centers of the crustal faults affecting the target site, while the magenta and the green regions are the slab models of the Hellenic and Calabrian arc respectively. Blue circles are the geometrical centers of the near-field sources, as detected in step (3b) (see text). The inset highlights the offshore points along the $50m$ isobath (red points). The blue rectangle within the zoom is the area displayed in the bottom panel. b) Zoom on the Milazzo oil refinery, with the position of the 95 points at the edges of the storage tanks (red points).

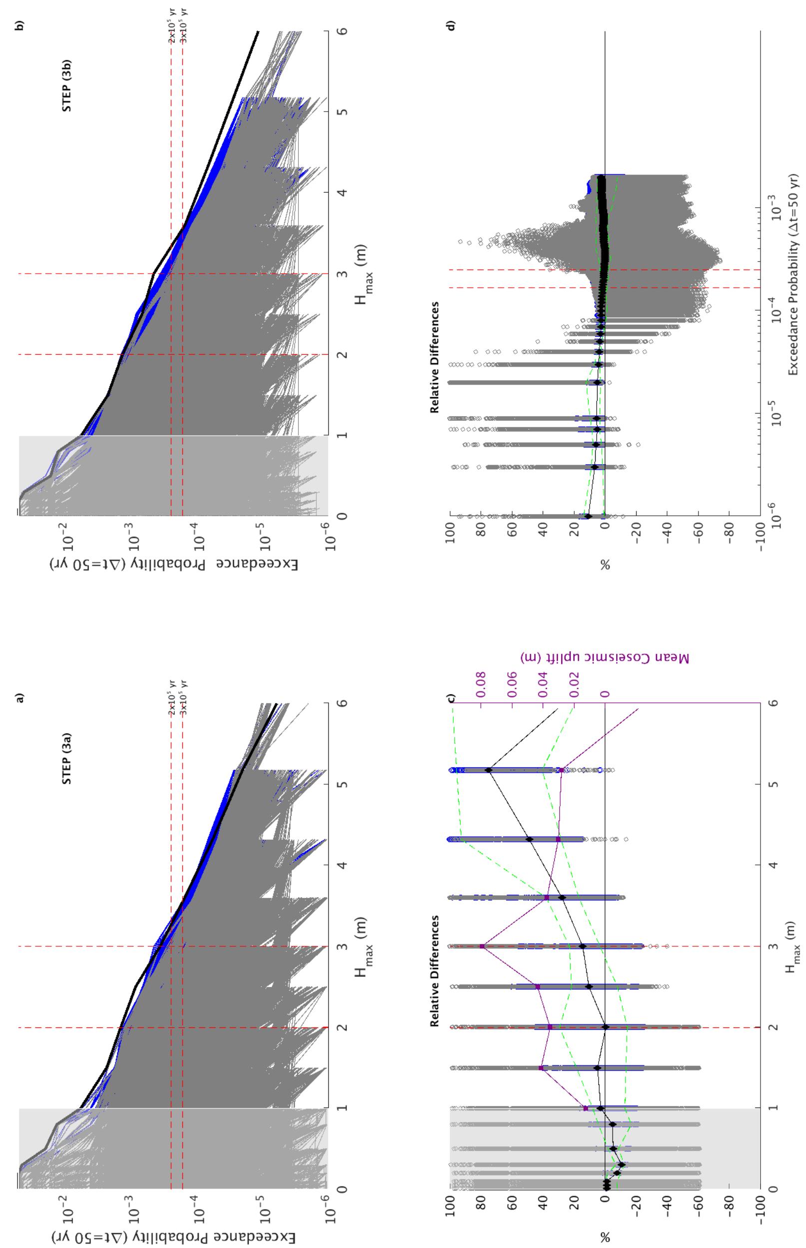

Figure 3. a) Mean hazard curves for H_{max} at all points within the highest resolution grid, as obtained from step (3a) of the SPTHA procedure (see text and Fig. 1). Grey and blue colors refer to inland and offshore points, respectively. The bold black line represents the envelope of the curves from step (3b). Red dashed lines represent the values used to obtain probability (Fig. 4) and hazard (Fig. 5) inundation maps. b) Same as a) but using step (3b). The bold black line is the envelope of the curves from step (3a). c) Relative differences in terms of exceedance probability (in $50yr$) as a function of H_{max}, computed as $[(3a)-(3b)]/(3b)$. The black line is the median of the point distribution; the green dashed lines correspond to the 16^{th} and 84^{th} percentile. The MU, namely the mean uplift on a random point along the coastline (see text) is also superimposed (purple line). d) Same as c) but in terms of H_{max} as a function of the exceedance probability (in $50yr$).

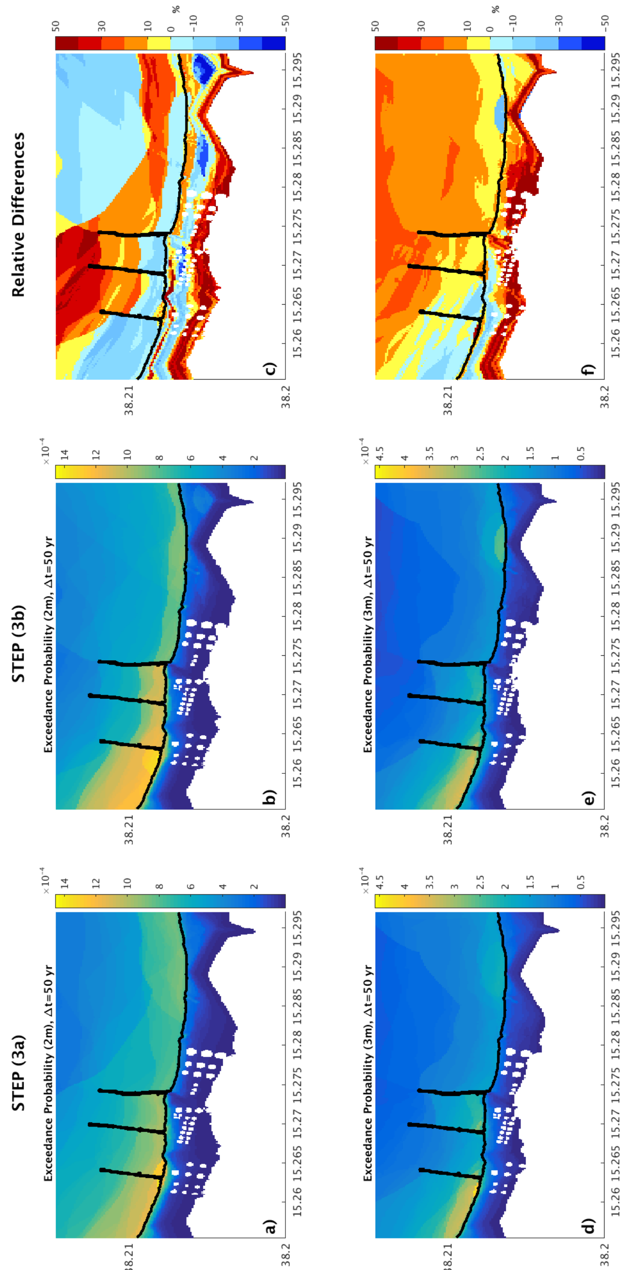

Figure 4. Probability maps (inner grid) for H_{max} derived from the hazard curves in Fig. 3 at two different thresholds ($2m$, $3m$) for step (3a) and (3b) and relative differences computed as $[(3a) - (3b)]/(3b)$.

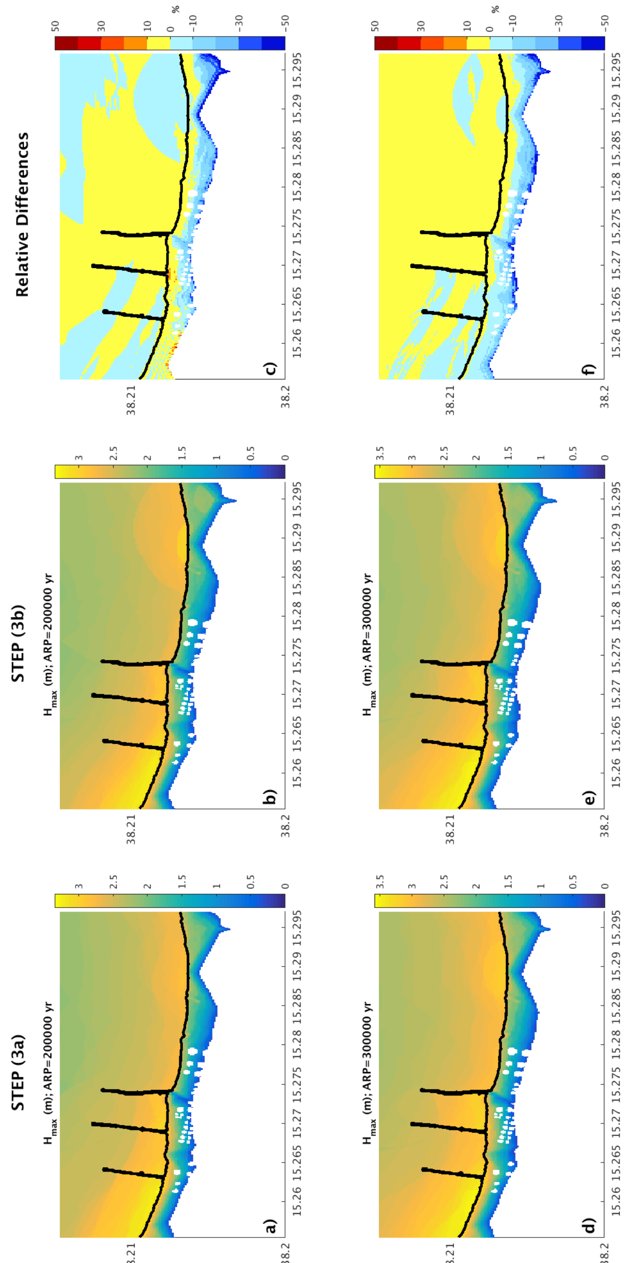

Figure 5. Hazard maps (inner grid) for H_{max} derived from the hazard curves in Fig. 3 at two different ARPs ($2 \times 10^5 yr$, $3 \times 10^5 yr$) for step (3a) and (3b) and relative differences computed as $[(3a) - (3b)] / (3b)$.

Supplementary Material

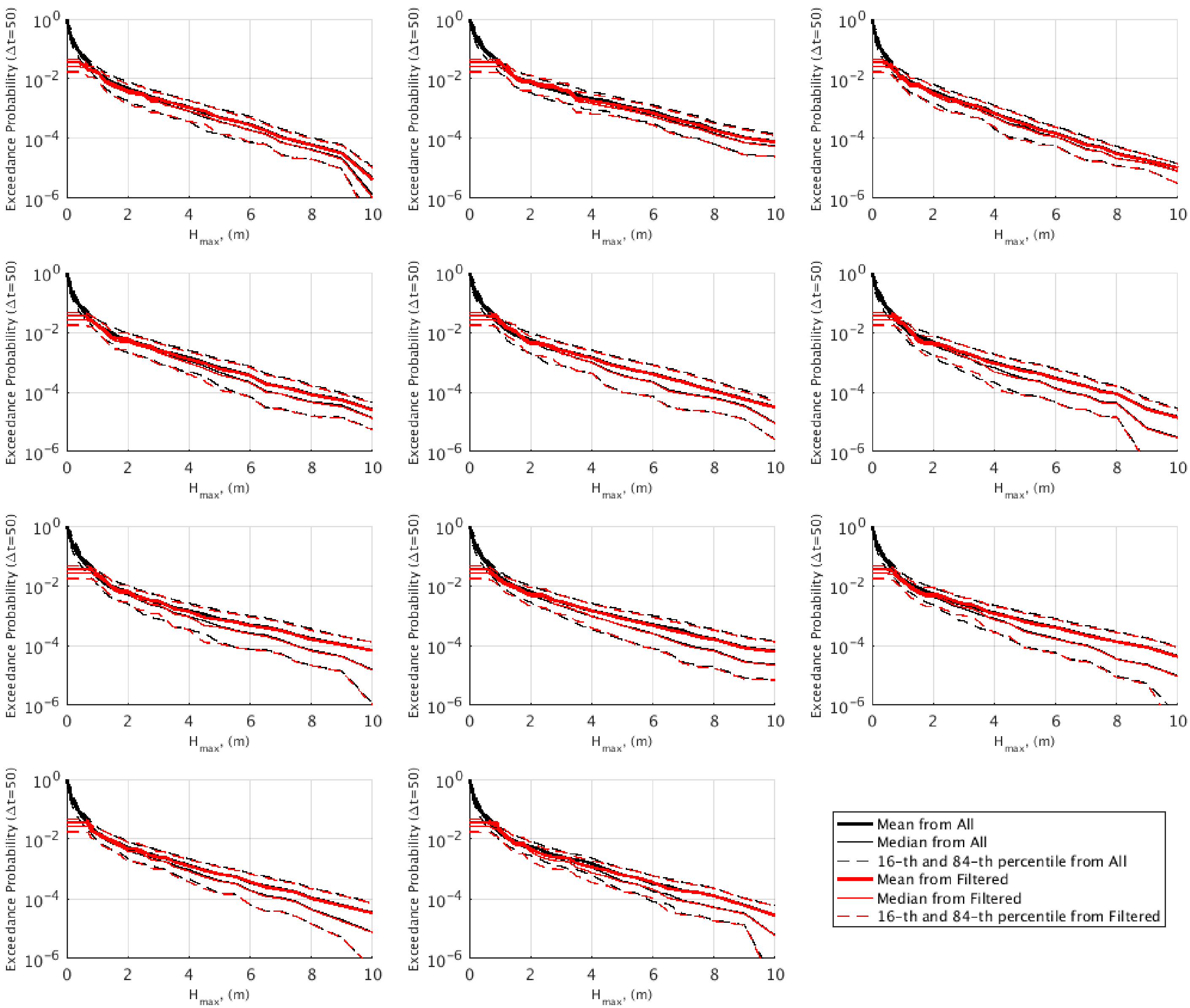

Figure S1. Offshore hazard curves at the 11 control points as obtained from the original and the filtered set of sources. The mean as well as some significant quantiles of the epistemic uncertainty are shown.

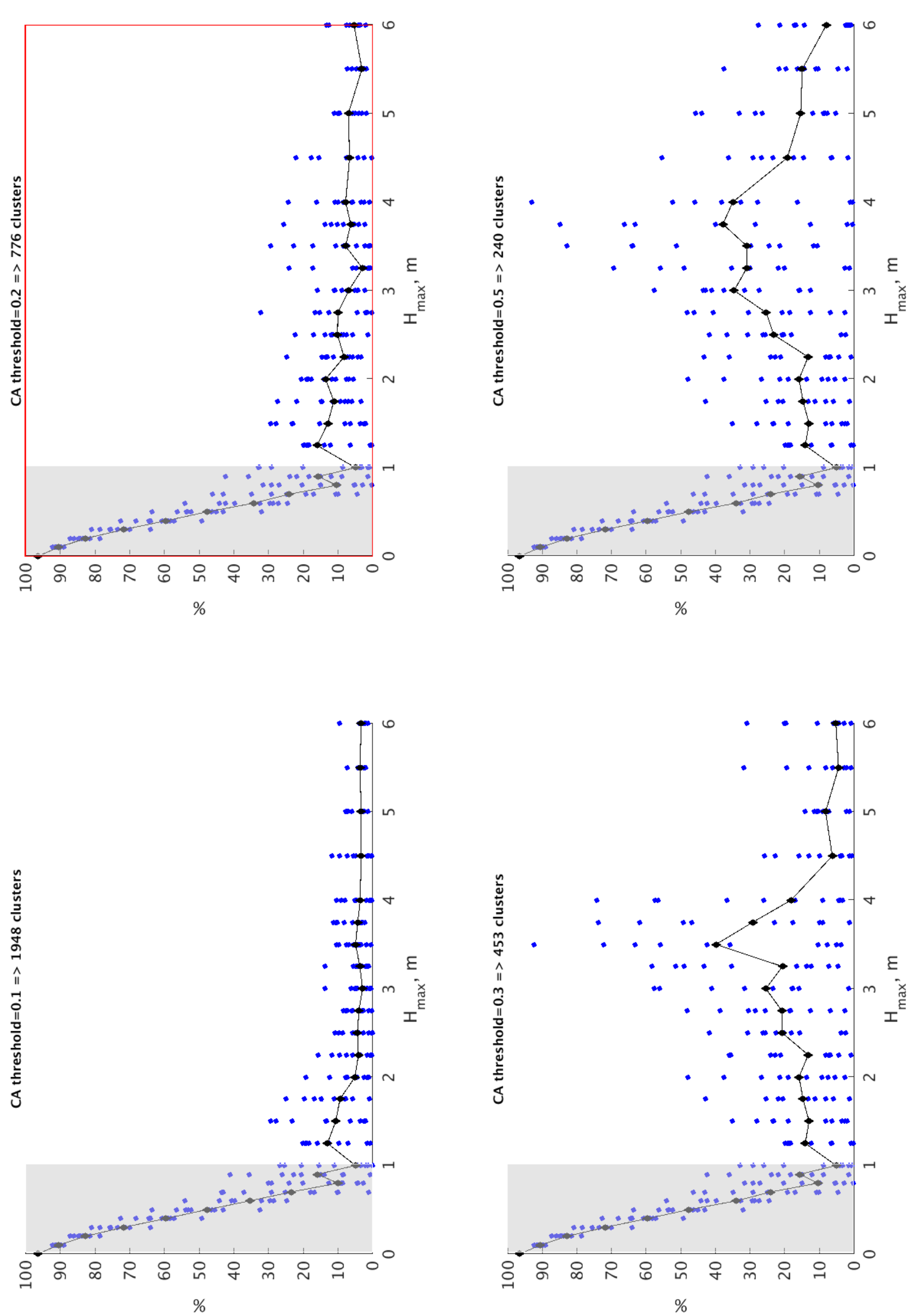

Figure S2. Sensitivity analysis (for step (3a)) concerning the cluster analysis threshold, showing the percentage differences between the offshore hazard curves computed from the original and the filtered set of sources, for different tsunami intensities. The higher is the threshold, i.e. the stronger is the imposed constraint, the more accurate is the clustering, to the detriment of the number of clusters. On the contrary, lower thresholds lead to less clusters but enlarge the errors. The red box corresponds to the value adopted in this study.

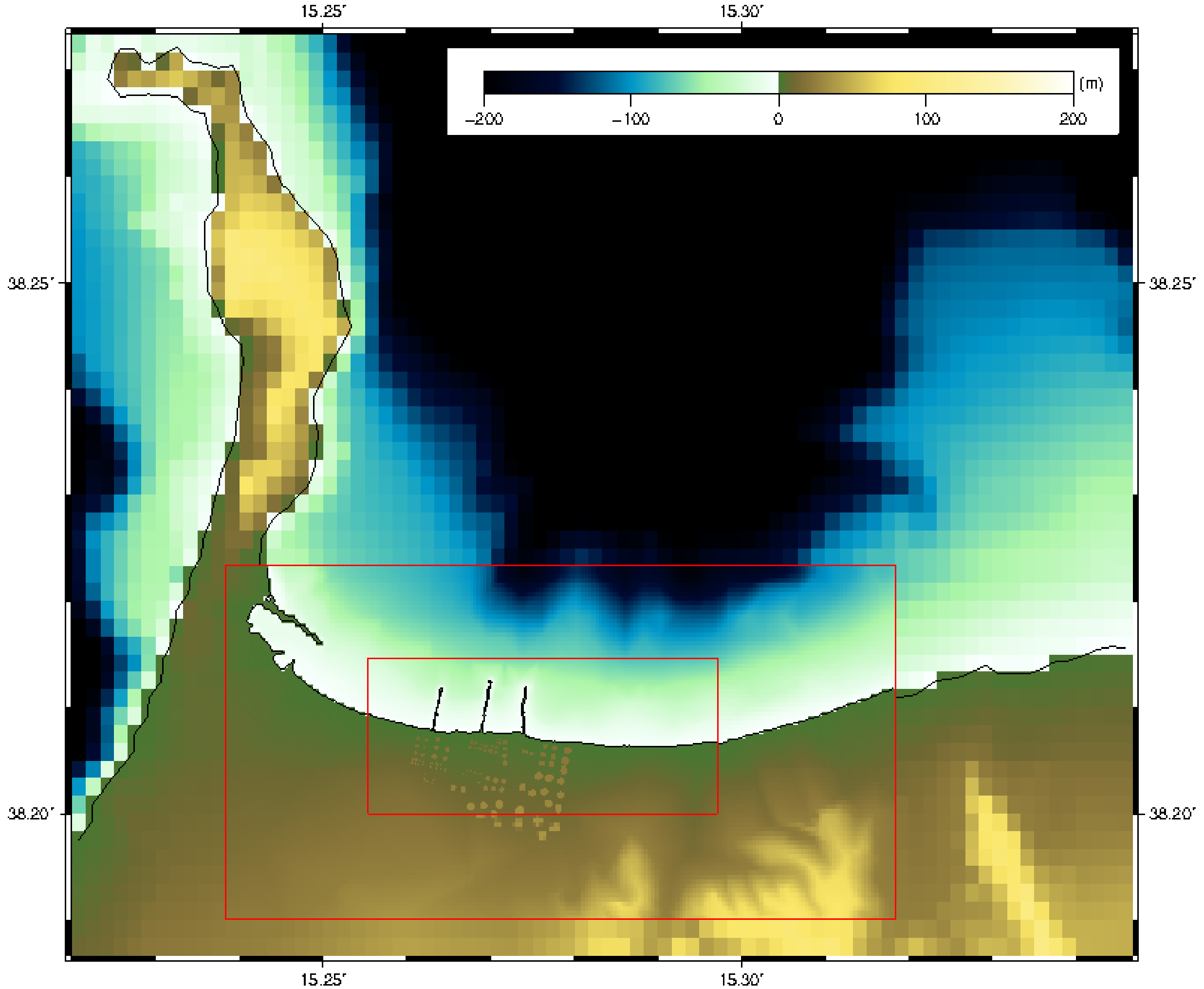

Figure S3. Close-up view of the topo-bathymetric nested grids used for tsunami simulations, with gradually increasing resolution (0.1, 0.025, 0.00625 arc-min). The domain of the outer grid (0.4 arc-min) is the one showed in Fig. 2 of the manuscript.

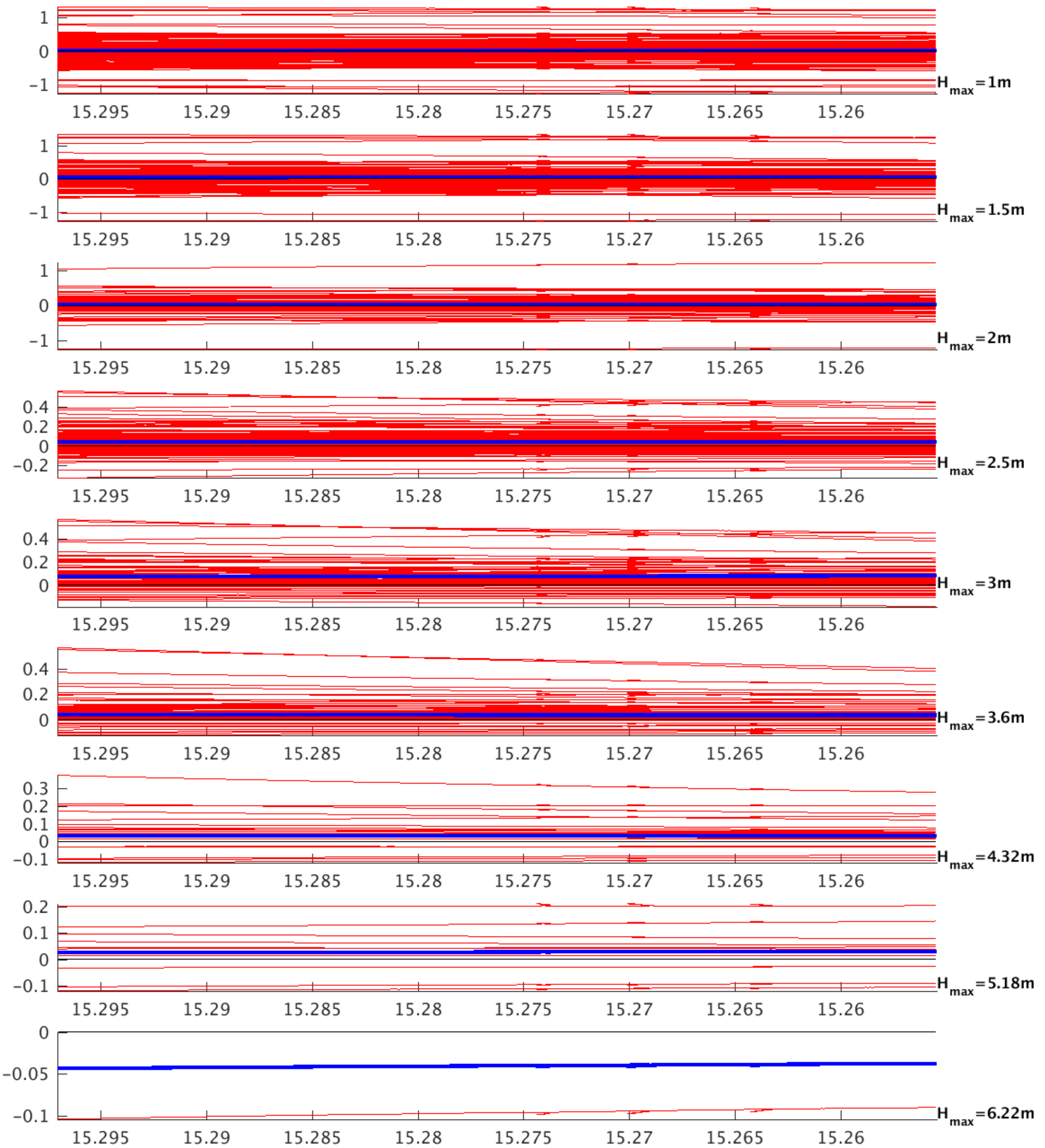

Figure S4. Red lines: coseismic displacements along the coastline of the higher resolution grid produced by each representative scenario contributing to different H_{max} values ($\geq 1m$). Blue lines: weighted averages on all the scenarios.

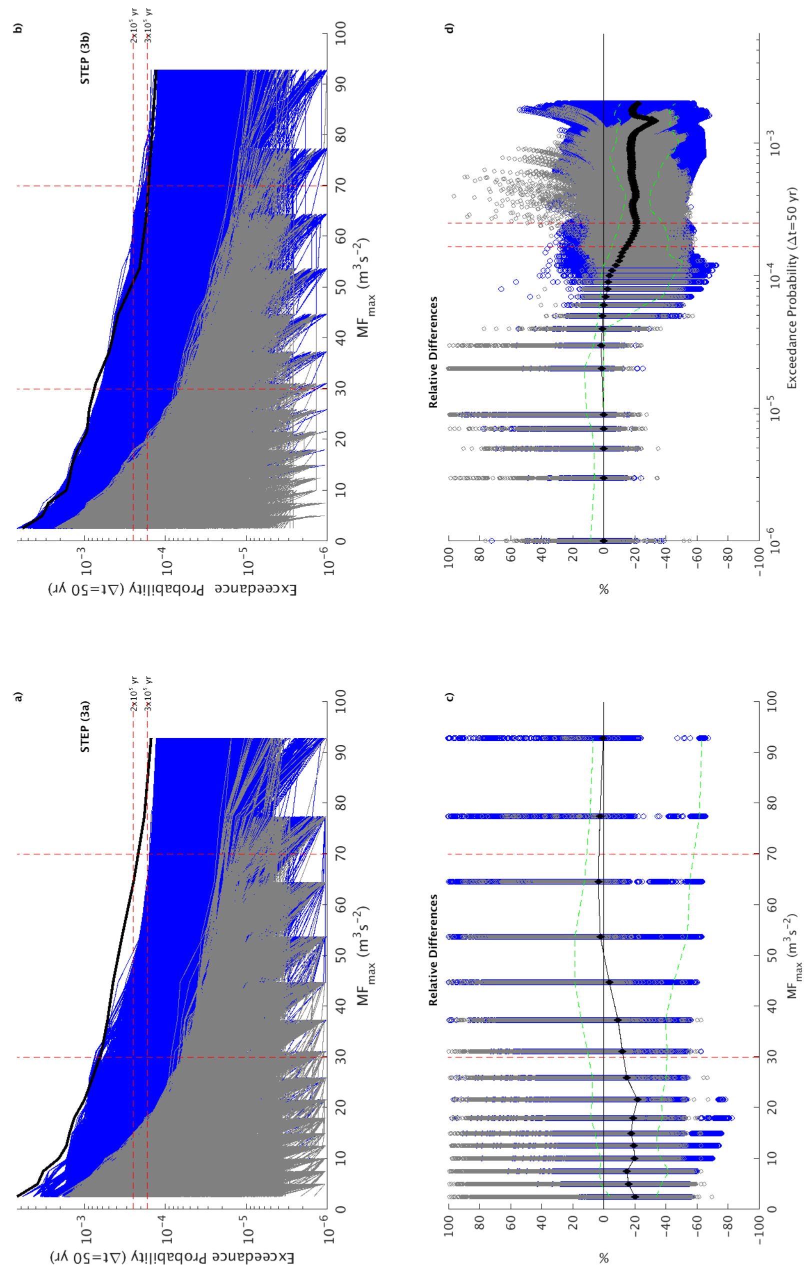

Figure S5. a) Mean hazard curves for MF_{max} at all points within the highest resolution grid, as obtained from step (3a) of the SPTHA procedure (see text and Fig. 1). Grey and blue colors refer to inland and offshore points, respectively. The bold black line represents the envelope of the curves from step (3b). Red dashed lines represent the values used to obtain probability (Fig. S6) and hazard (Fig. S7) inundation maps. b) Same as a) but using step (3b). The bold black line is the envelope of the curves from step (3a). c) Relative differences in terms of exceedance probability (in $50yr$) as a function of MF_{max}, computed as $[(3a) - (3b)] / (3b)$. The black line is the median of the point distribution; the green dashed lines correspond to the 16^{th} and 84^{th} percentile. d) Same as c) but in terms of MF_{max} as a function of the exceedance probability (in $50yr$).

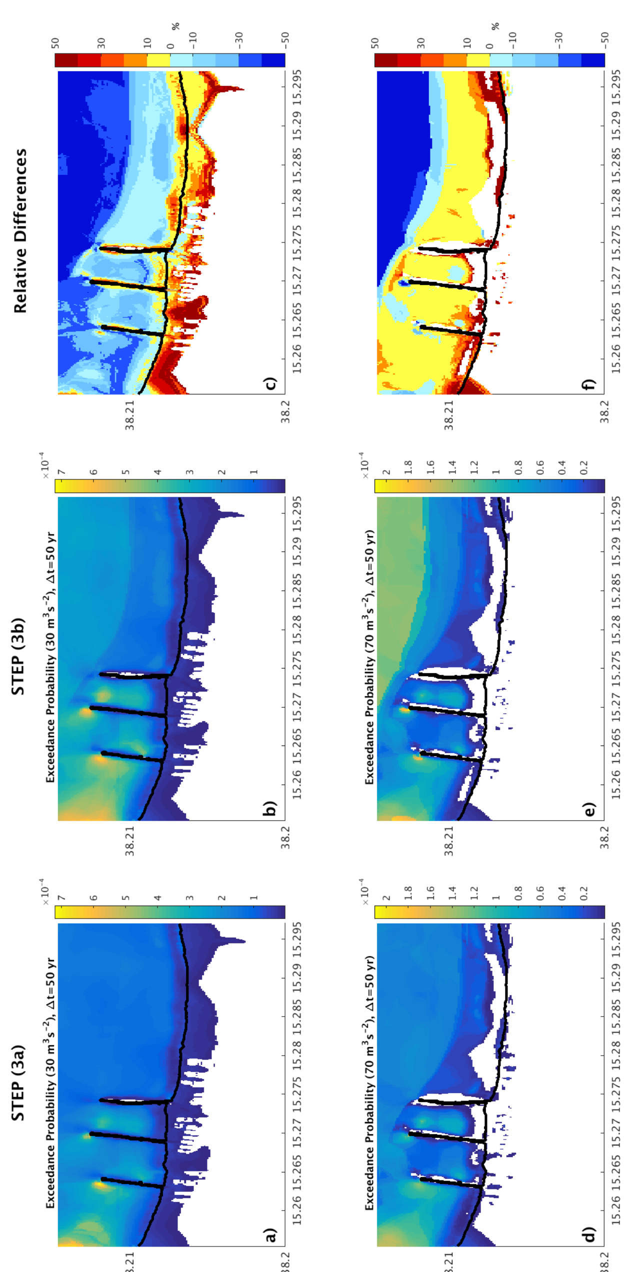

Figure S6. Probability maps (inner grid) for MF_{max} derived from the hazard curves in Fig. S5 at two different thresholds ($30m^3s^{-2}$, $70m^3s^{-2}$) for step (3a) and (3b) and relative differences computed as $[(3a)-(3b)]/(3b)$.

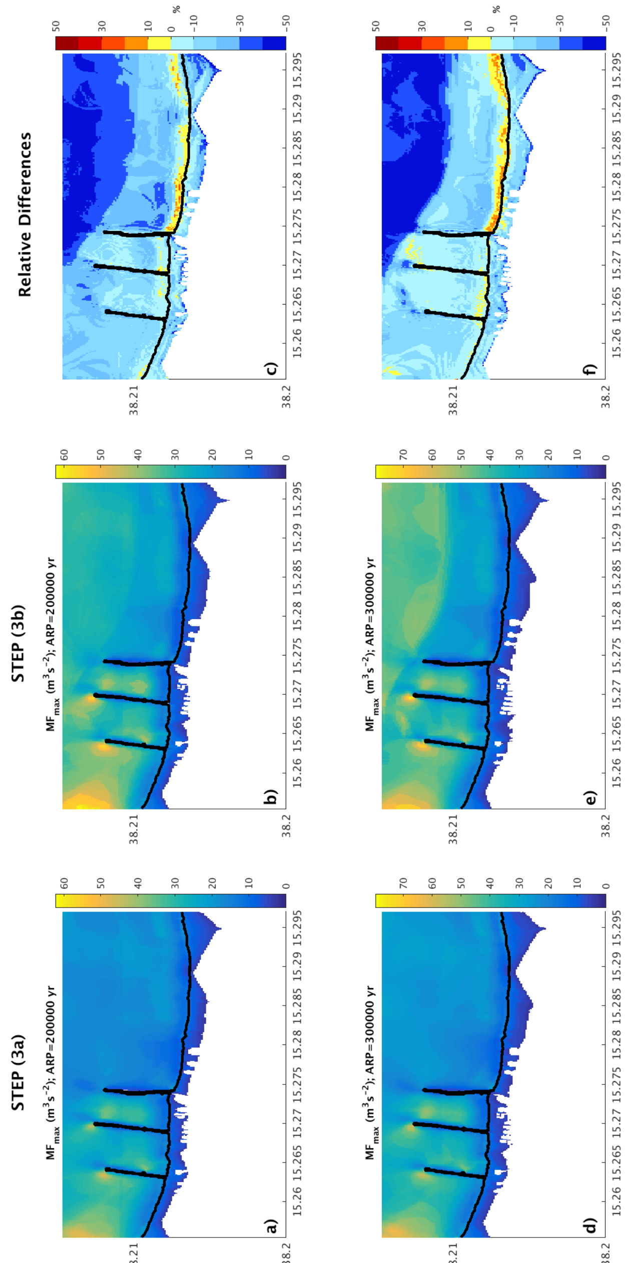

Figure S7. Hazard maps (inner grid) for MF_{max} derived from the hazard curves in Fig. S5 at two different ARPs ($2 \times 10^5 yr$, $3 \times 10^5 yr$) for step (3a) and (3b) and relative differences computed as $[(3a) - (3b)]/(3b)$.